Lepton-nucleus scattering: from the quasi-elastic to the DIS region

Noemi Rocco

Brookhaven Neutrino Theory Virtual Seminars
Argonne National Laboratory
August 19, 2020

In Collaboration with: O. Benhar, J. Carlson, S. Gandolfi, J. Isaacson, W. Jay, T.S.H. Lee, A. Lovato, P. Machado, S.X. Nakamura, T. Sato, R. Schiavilla

Addressing Neutrino-Oscillation Physics

$$P_{\nu_\mu \to \nu_e}(E, L) \sim \sin^2 2\theta \sin^2\left(\frac{\Delta m^2 L}{4E}\right) \to \Phi_e(E, L)/\Phi_\mu(E, 0)$$

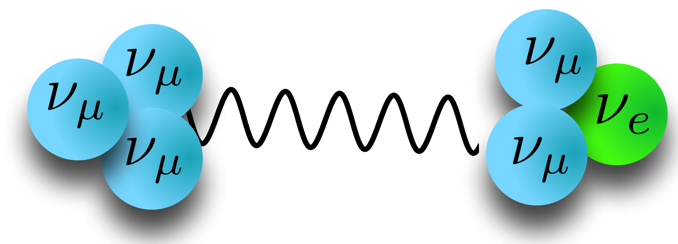

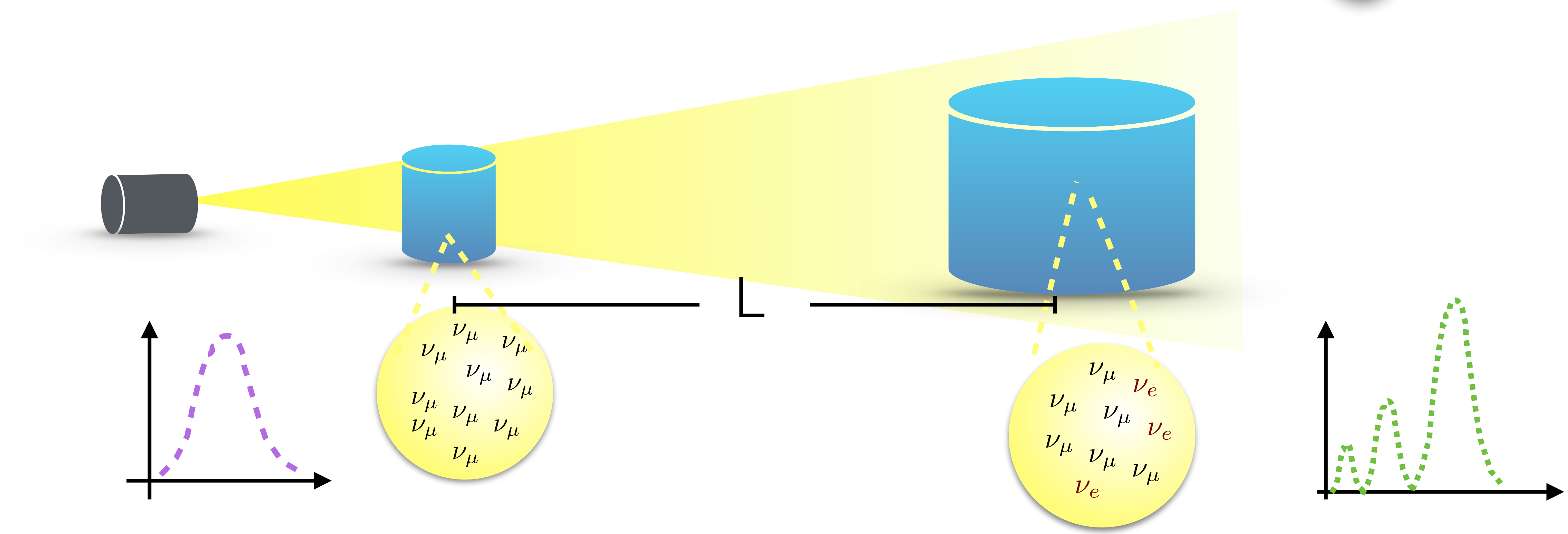

Detectors measure the neutrino interaction rate:

$$N_e(E_{\text{rec}}, L) \propto \sum_i \Phi_e(E, L)\sigma_i(E) f_{\sigma_i}(E, E_{\text{rec}})dE$$

Reconstructed
ν energy

Cross Section

Smearing
matrix

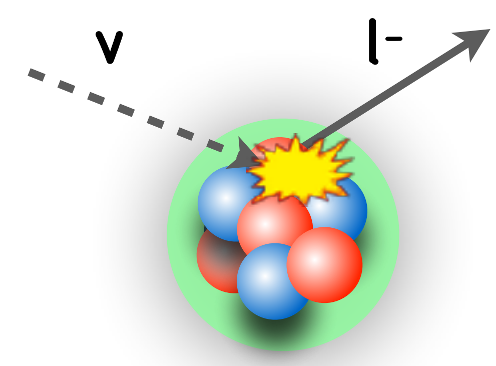

A quantitative knowledge of σ(E) and f_σ(E) is crucial to precisely extract ν oscillation parameters

To study neutrinos we need nuclei

? Where does Nuclear Physics come into play

Number of Interactions = $\underbrace{\sigma}_{\text{Cross Section}} \times \underbrace{\Phi}_{\text{Neutrino Flux}} \times \underbrace{N}_{\text{\# Targets}}$

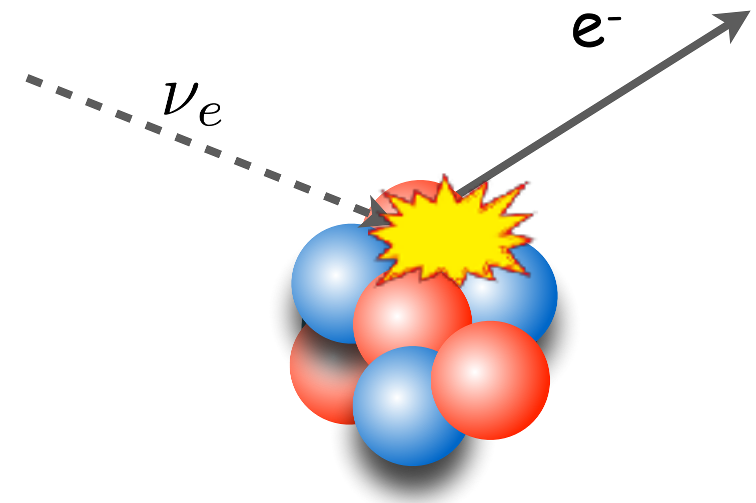

Utilize heavy target in neutrino detectors to maximize interactions→ understand nuclear structure

Carbon

NOvA

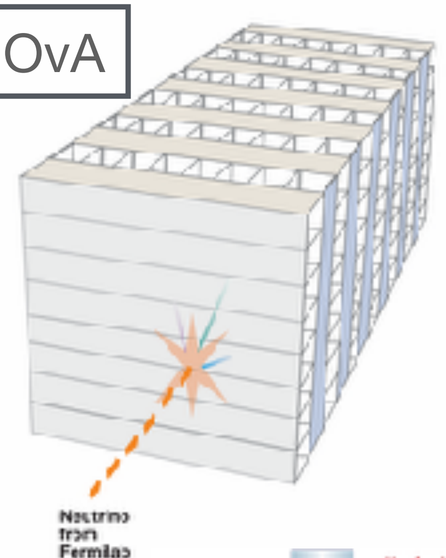

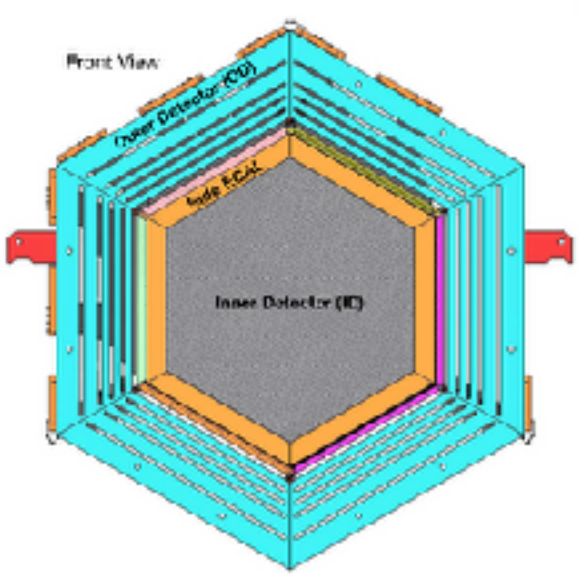

MINERvA

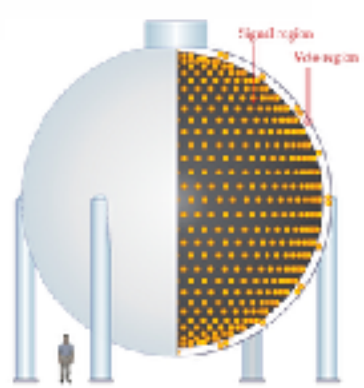

MiniBooNE

Liquid Argon

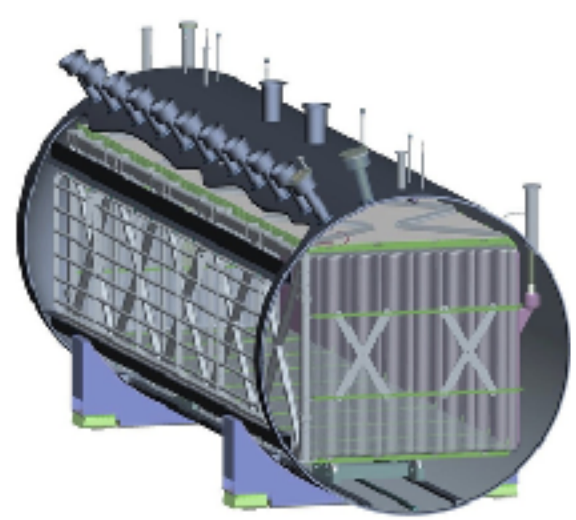

MicroBooNE

Icarus

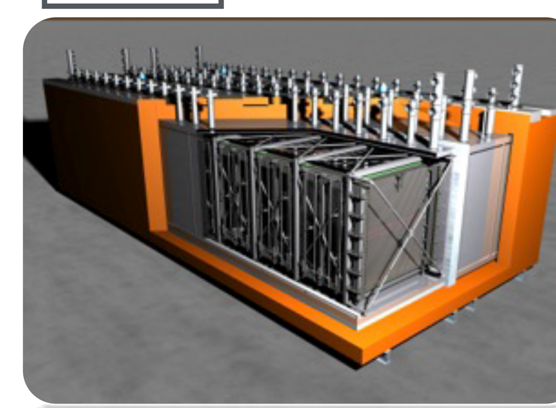

DUNE

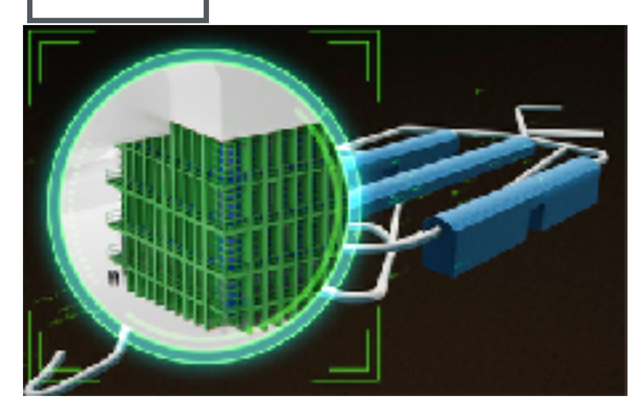

Outline of the talk

1st Part of the Presentation

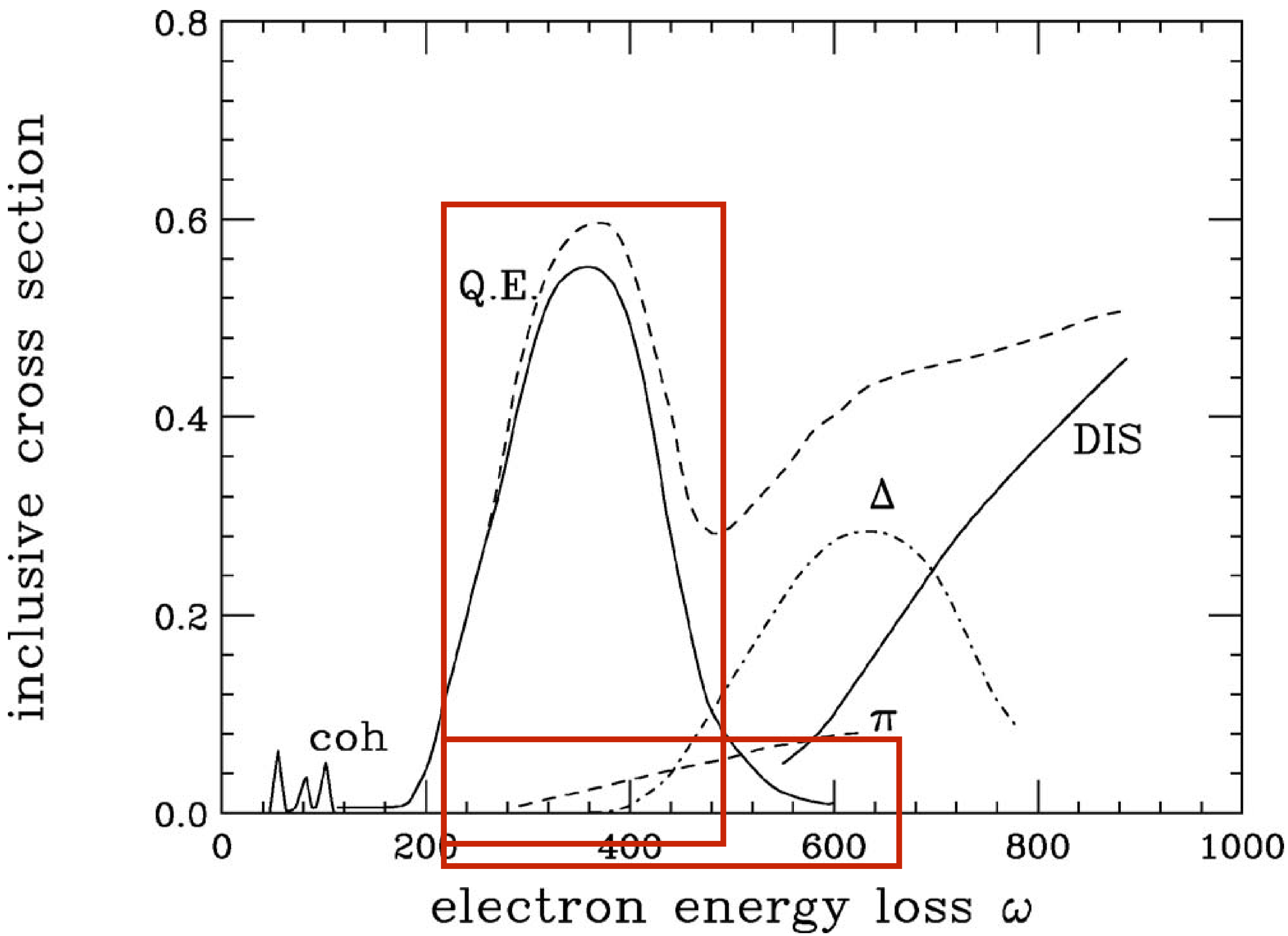

- Ab-initio calculations (GFMC)—able to describe how nuclei emerge starting from neutron and proton interactions—provide an accurate predictions of the QE region including one- and two-body currents

Quasielastic scattering on a nucleus:

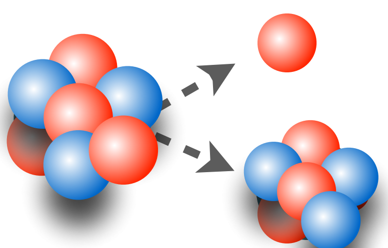

Outline of the talk

2nd Part of the Presentation

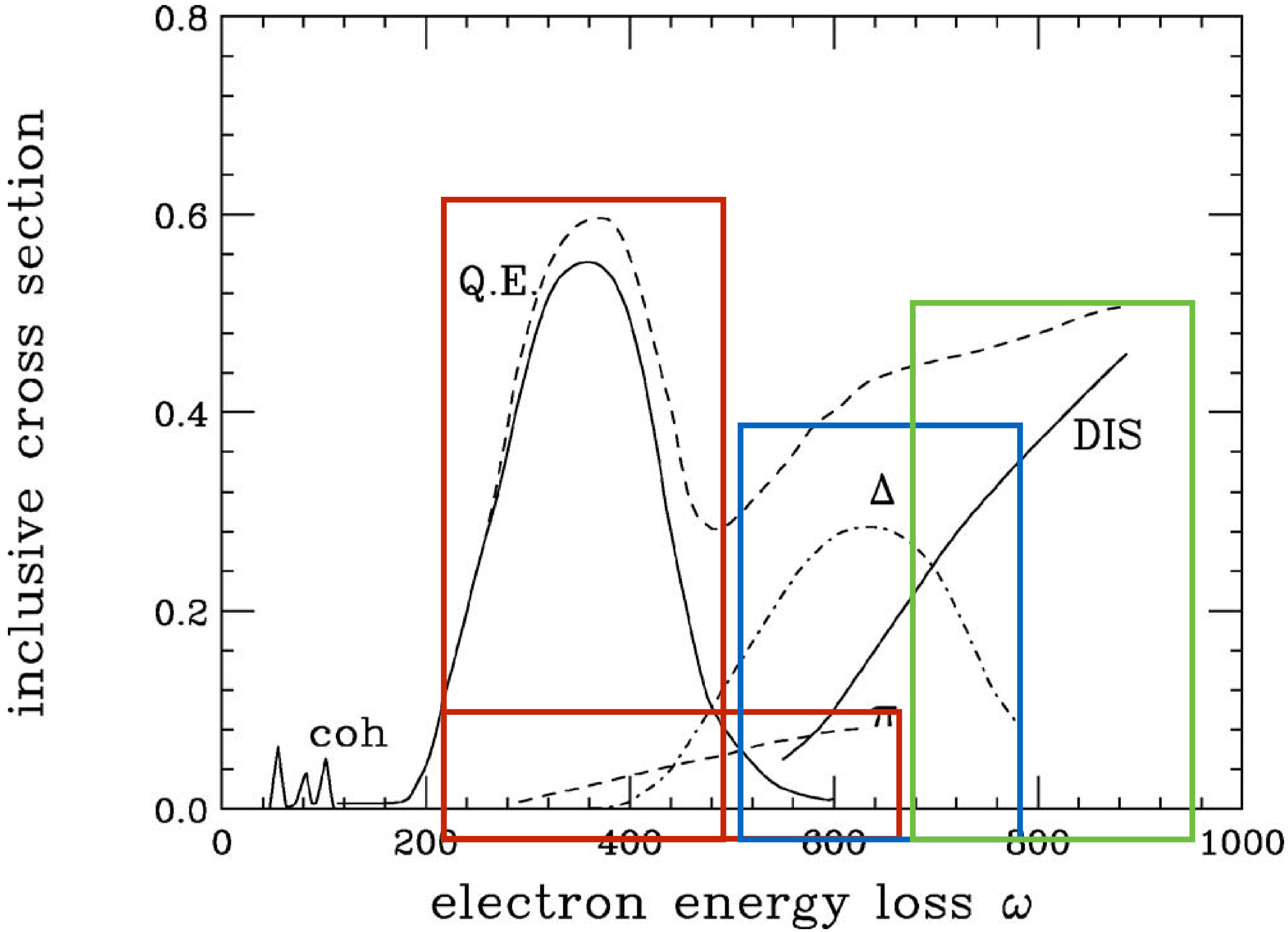

- More approximate approach: Extended Factorization scheme + Semi-phenomenological SF have been introduced to tackle QE, dip and π-production regions.

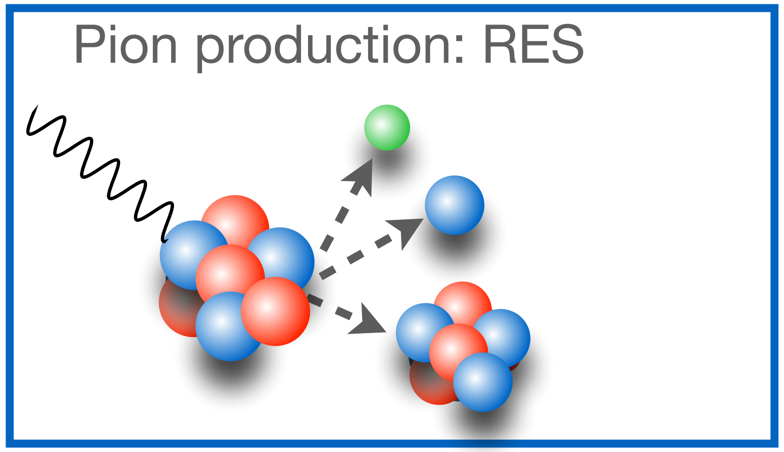

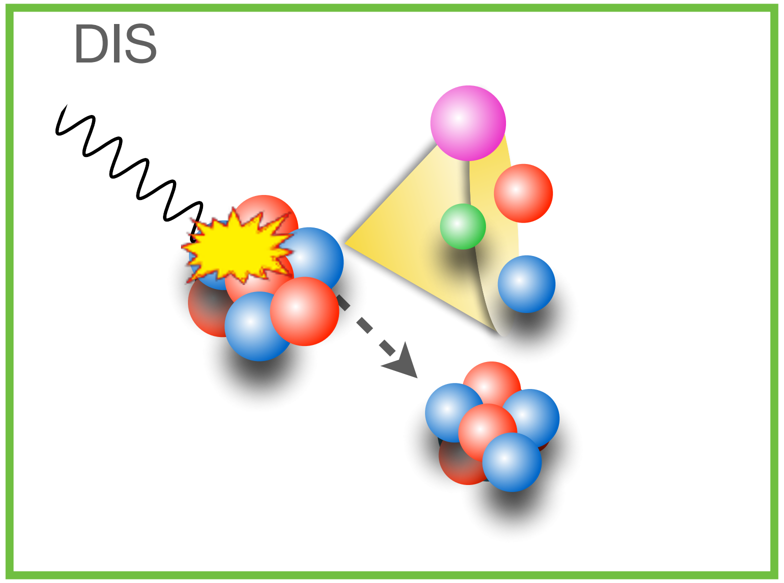

Outline of the talk

3nd Part of the Presentation

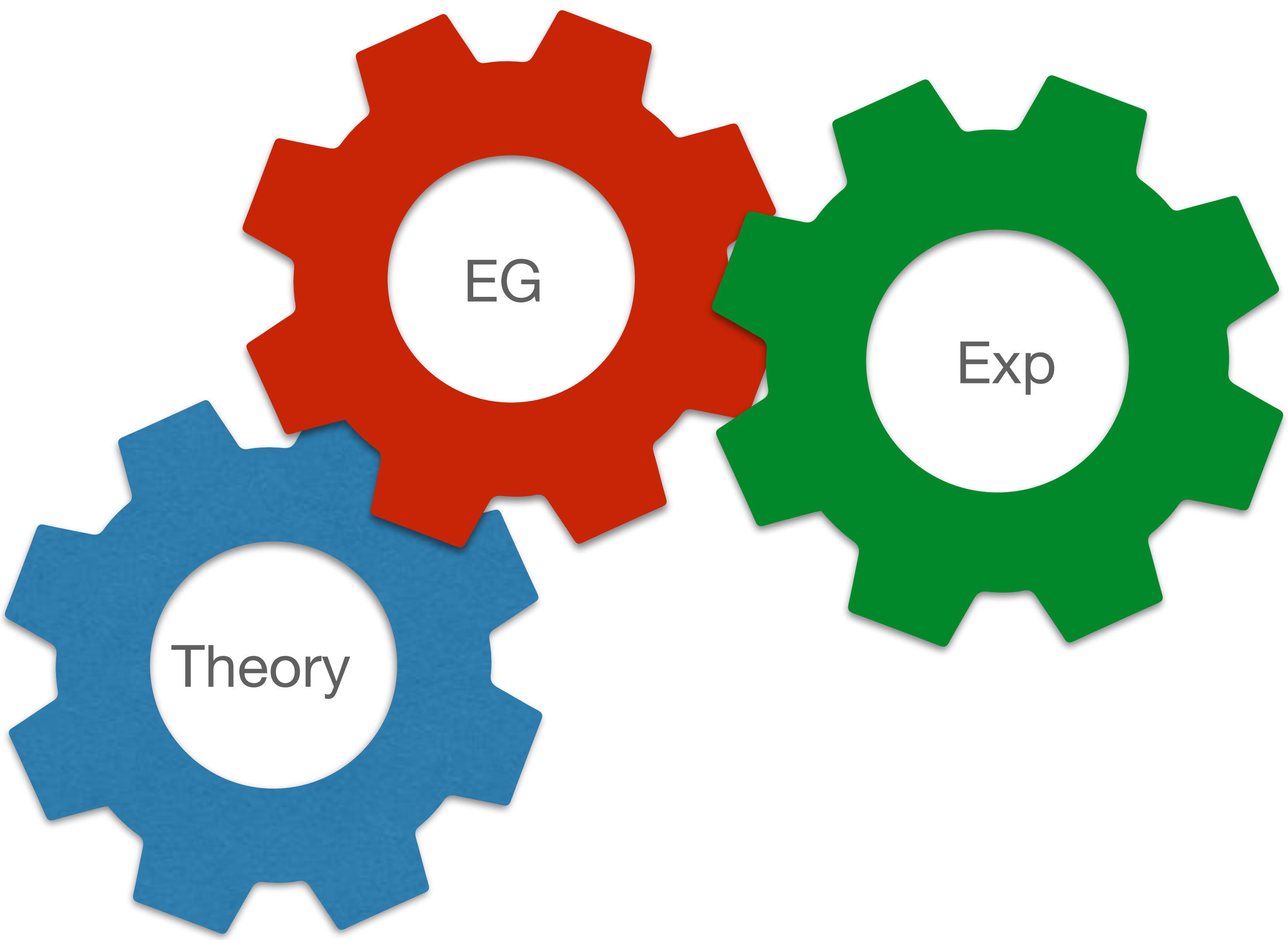

Synergistic effort among these three components:

what we are doing / plan to do for the event-generator component

Theory of lepton-nucleus scattering

The cross section of the process in which a lepton scatters off a nucleus is given by

$$d\sigma \propto L^{\alpha\beta} R_{\alpha\beta}$$

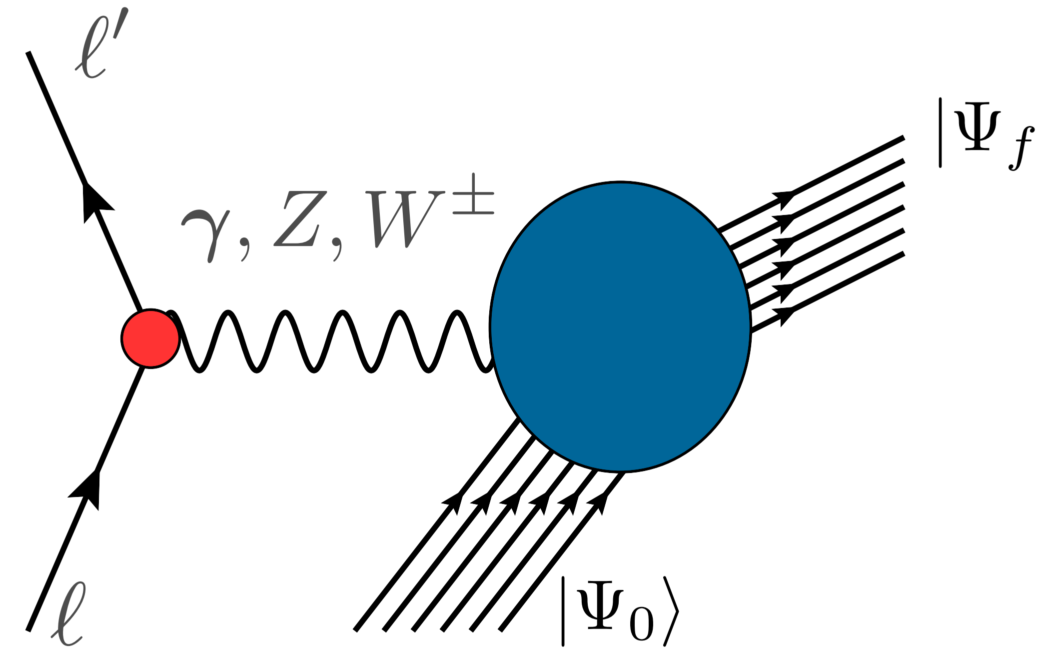

Nuclear response to the electroweak probe:

$$R_{\alpha\beta}(\omega, \mathbf{q}) = \sum_f \langle 0 | J_\alpha^\dagger(\mathbf{q}) | f \rangle \langle f | J_\beta(\mathbf{q}) | 0 \rangle \delta(\omega - E_f + E_0)$$

The initial and final wave functions describe many-body states:

$$|0\rangle = |\Psi_0^A\rangle \ , |f\rangle = |\Psi_f^A\rangle, |\psi_p^N, \Psi_f^{A-1}\rangle, |\psi_k^\pi, \psi_p^N, \Psi_f^{A-1}\rangle \ldots$$

One and two-body current operators

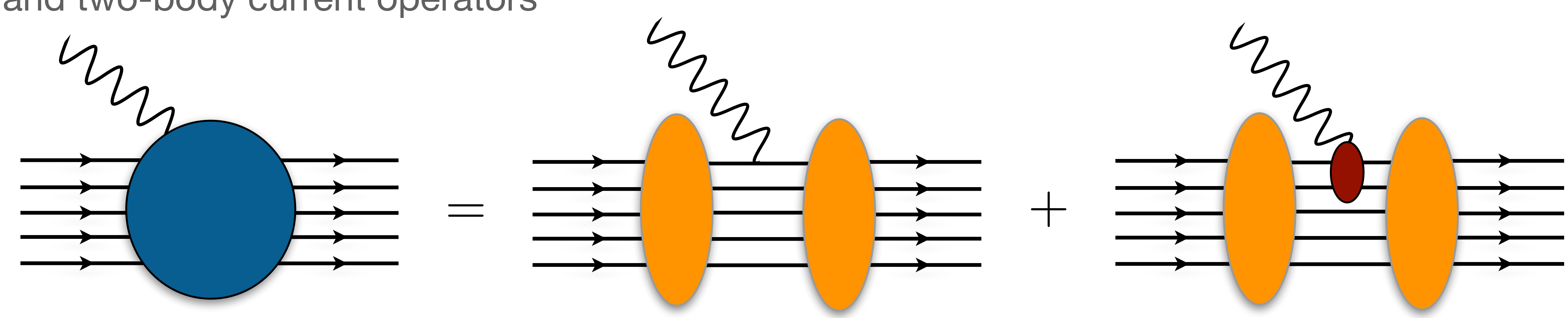

The basic model of nuclear theory

At low energy, the effective degrees of freedom are pions and nucleons:

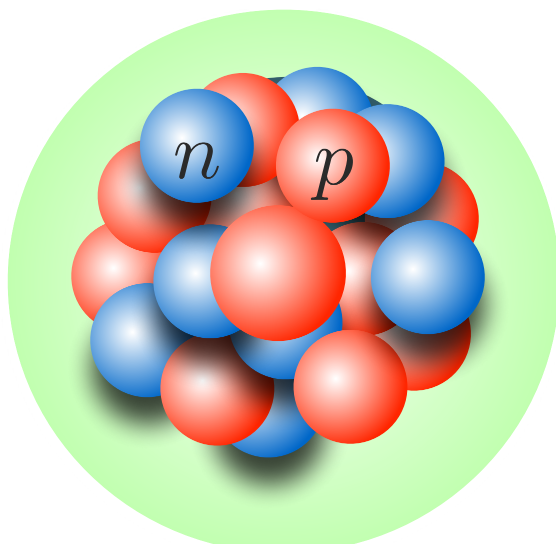

$$H = \sum_i \frac{\mathbf{p}_i^2}{2m} + \sum_{i<j} v_{ij} + \sum_{i<j<k} V_{ijk} + \ldots$$

1-body **2-body** **3-body**

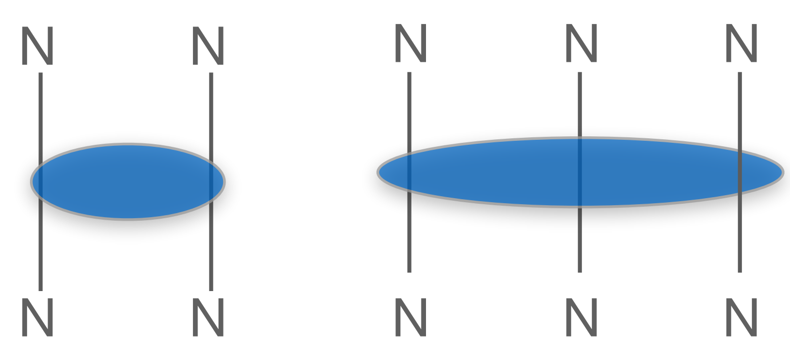

The electromagnetic current is constrained by the Hamiltonian through the **continuity equation**

$$\nabla \cdot \mathbf{J}_{\rm EM} + i[H, J^0_{\rm EM}] = 0 \qquad [v_{ij}, j_i^0] \neq 0$$

The above equation implies that the current operator includes one and two-body contributions

$$J^\mu(q) = \sum_i j_i^\mu + \sum_{i<j} j_{ij}^\mu + \ldots$$

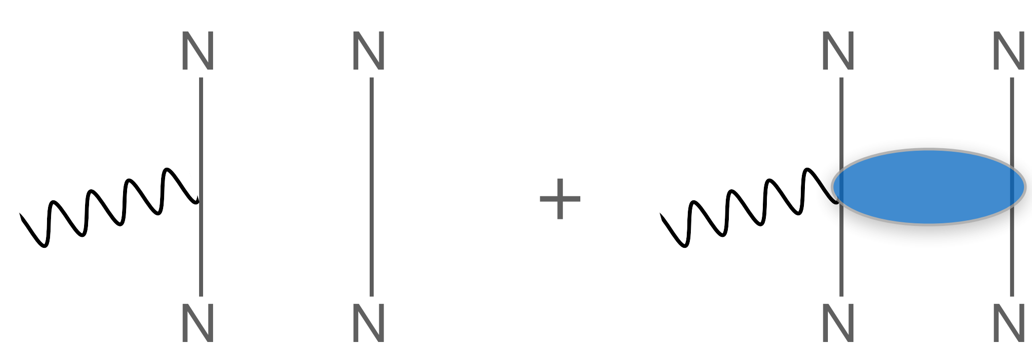

Quantum Monte Carlo approach

We want to solve the Schrödinger equation

$$H\Psi(\mathbf{R}; s_1 \ldots s_A, \tau_1 \ldots \tau_A) = E\Psi(\mathbf{R}; s_1 \ldots s_A, \tau_1 \ldots \tau_A)$$

Any trial wave function can be expanded in the complete set of eigenstates of the the Hamiltonian according to

$$|\Psi_T\rangle = \sum_n c_n |\Psi_n\rangle \qquad\qquad H|\Psi_n\rangle = E_n|\Psi_n\rangle$$

QMC techniques **projects out the exact lowest-energy state:** $e^{-(H-E_0)\tau}|\Psi_T\rangle \to |\Psi_0\rangle$

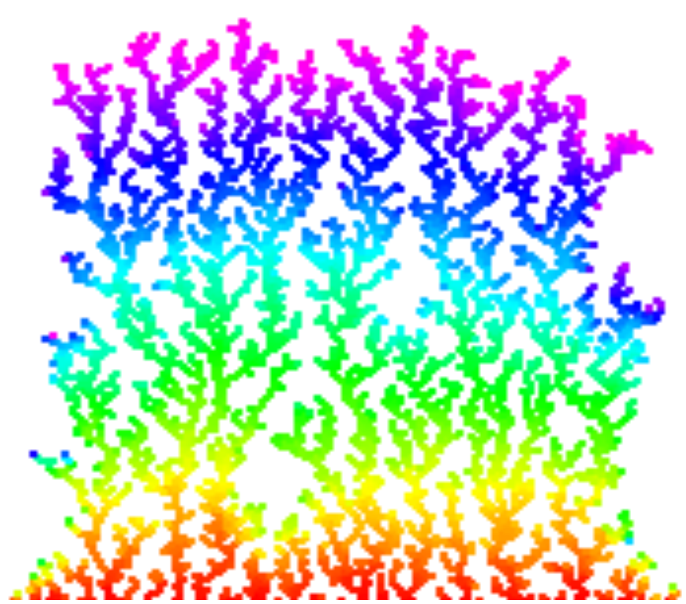

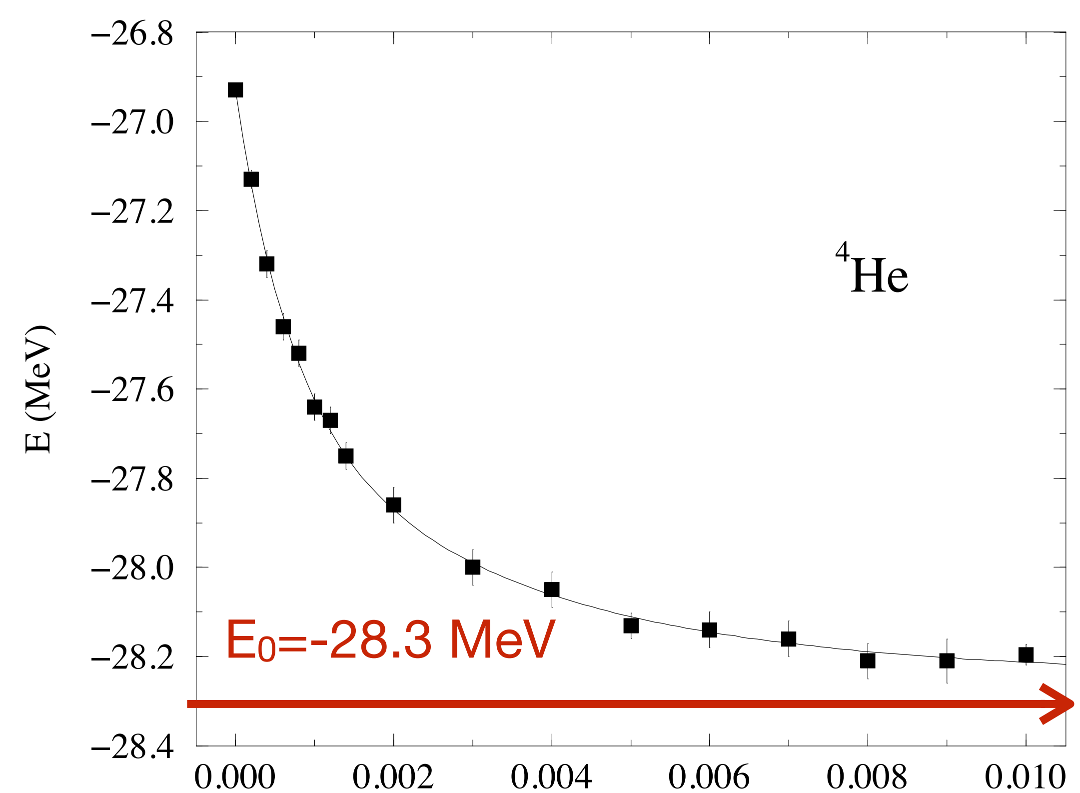

The system is cooled down by evolving it in time

✐ B. Pudliner et al., PRC **56**, 1720 (1997)

GFMC electron ^{4}He-cross sections

Virtually exact results for nuclear electroweak responses in the **quasi-elastic region** up to moderate values of **q**.
Initial and final state interactions fully accounted for.

Computational cost grows exponentially with the number of particles: currently limited to ^{12}C

N.R, W. Leidemann, et al PRC 97 (2018) no.5, 055501

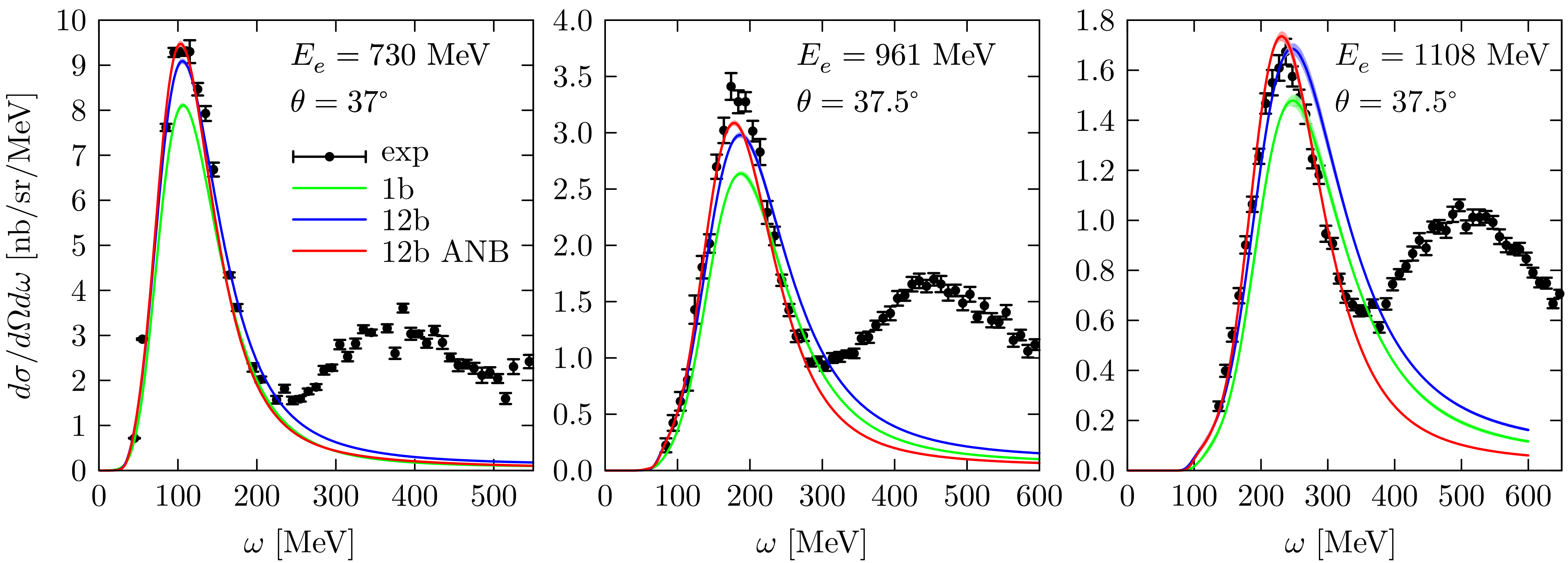

- Very good agreement in the quasielastic region when: one- and two-body currents are included
- Peak on the right: π production can not be described within this approach

GFMC CC ν_μ ^{12}C-cross sections

✐A.Lovato, NR et al, arXiv:2003.07710, PRX in press

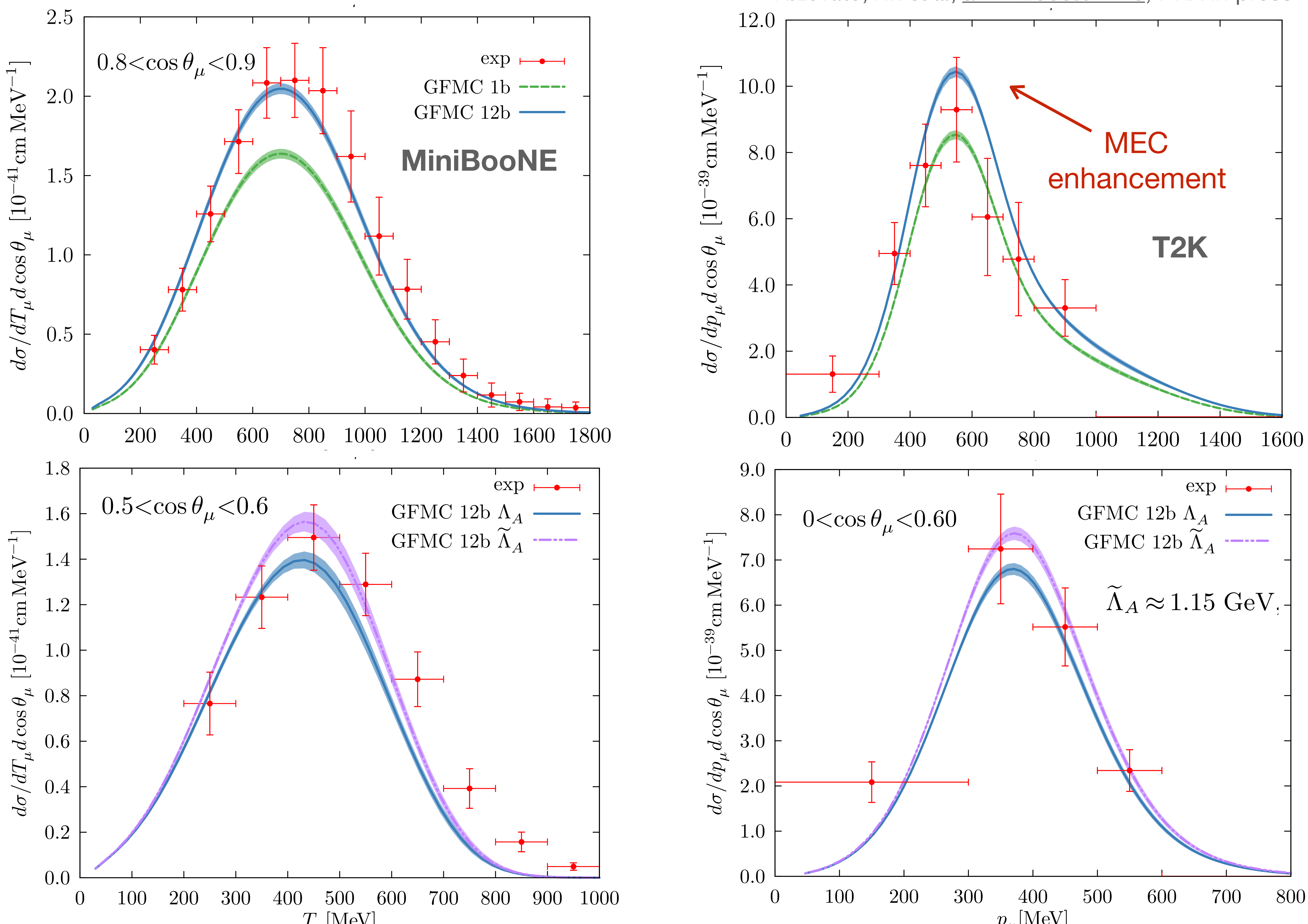

Addressing future precision experiments

- Liquid Argon TPC Technology

J.A. Formaggio and G.P. Zeller, Rev. Mod. Phys. 84 (2012)

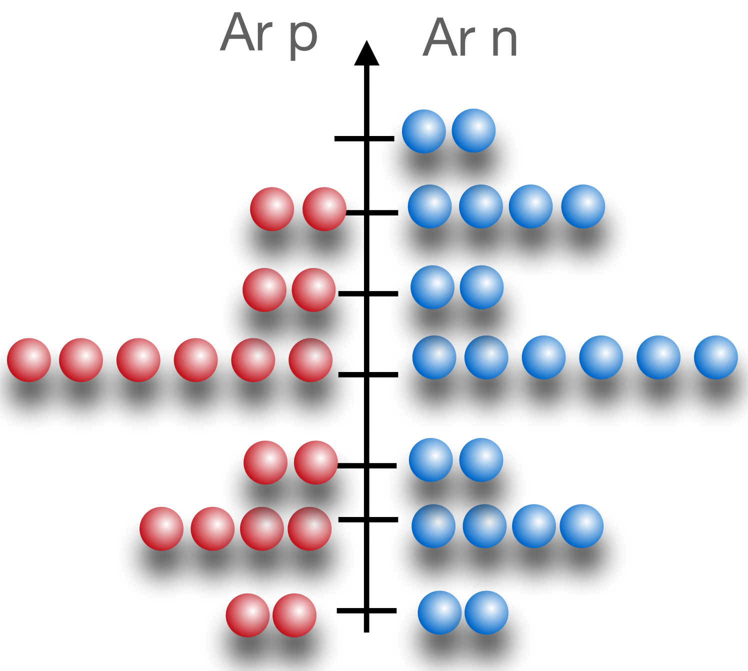

- Ar has a complicated structure, out of the reach of most of the ab initio methods

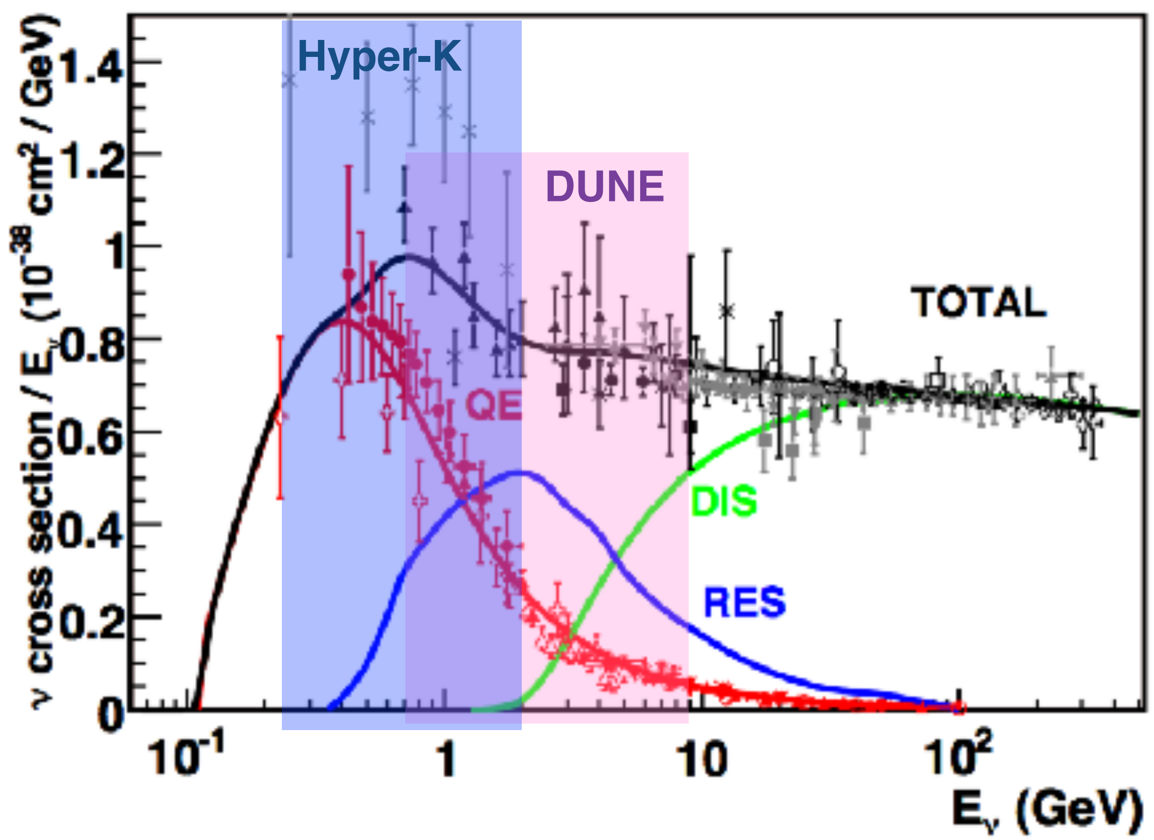

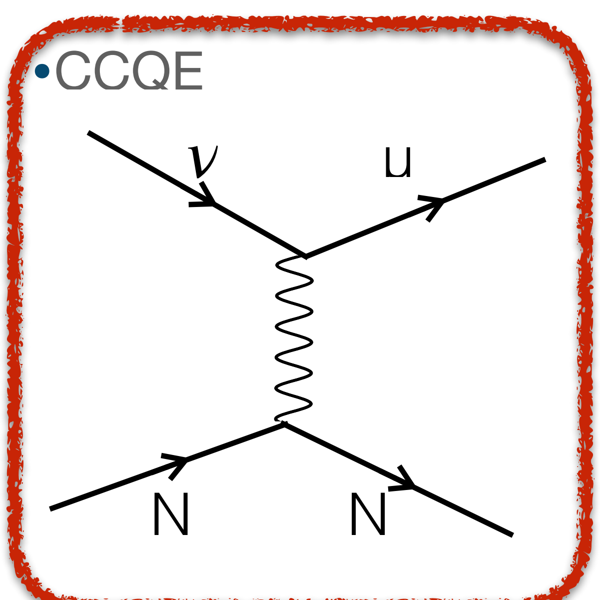

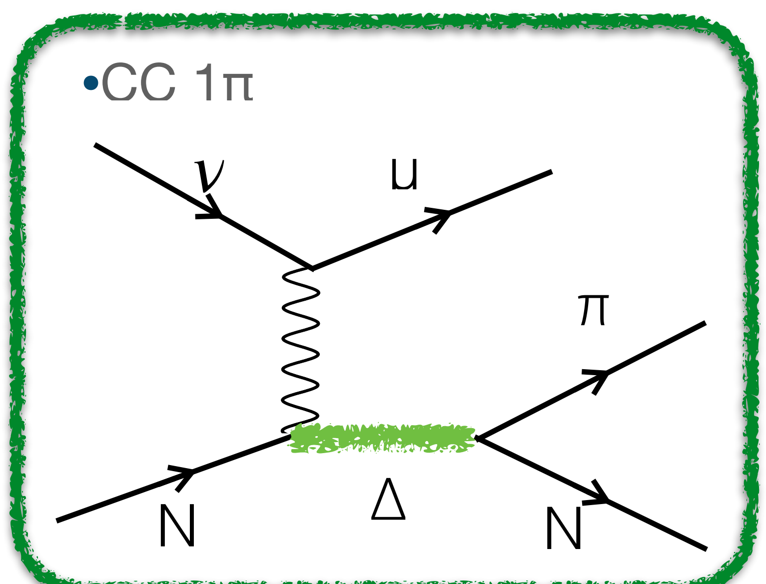

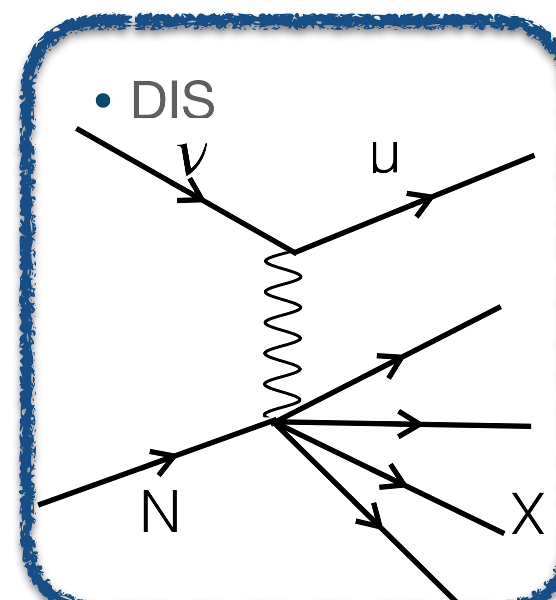

- The dominant reaction mechanism changes dramatically over the region of interest to oscillation experiment

Factorization Scheme and Spectral Function

For sufficiently large values of |**q**|, the **factorization scheme** can be applied under the assumptions

$$|\Psi_f\rangle \rightarrow |p\rangle \otimes |\Psi_f\rangle_{A-1}$$

$$J_\alpha = \sum_i j_\alpha^i$$

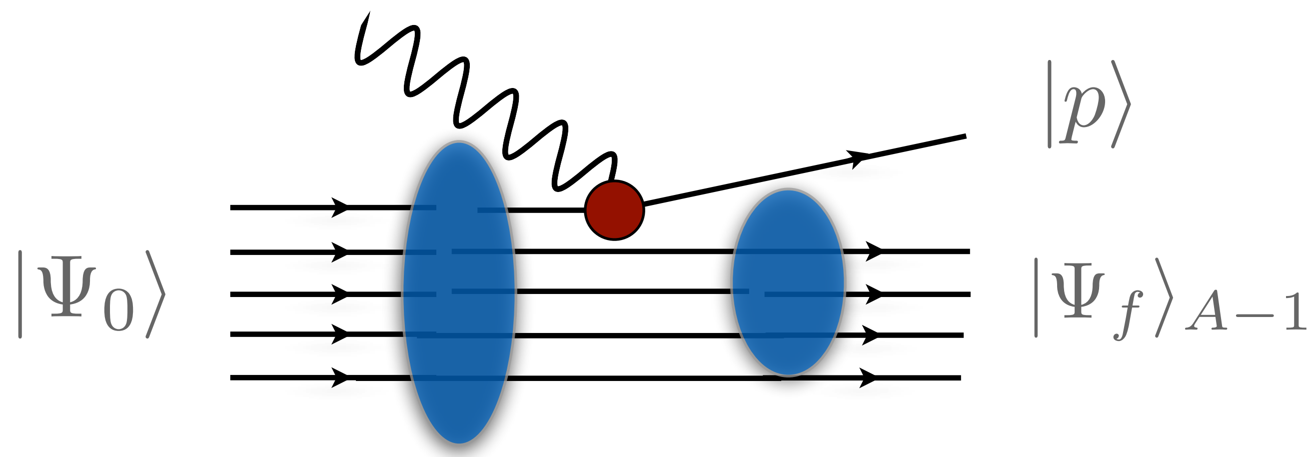

The nuclear cross section is given in terms of the one describing the interaction with individual bound nucleons

$$\boxed{d\sigma_A = \int dE d^3k \; d\sigma_N P(\mathbf{k}, E)}$$

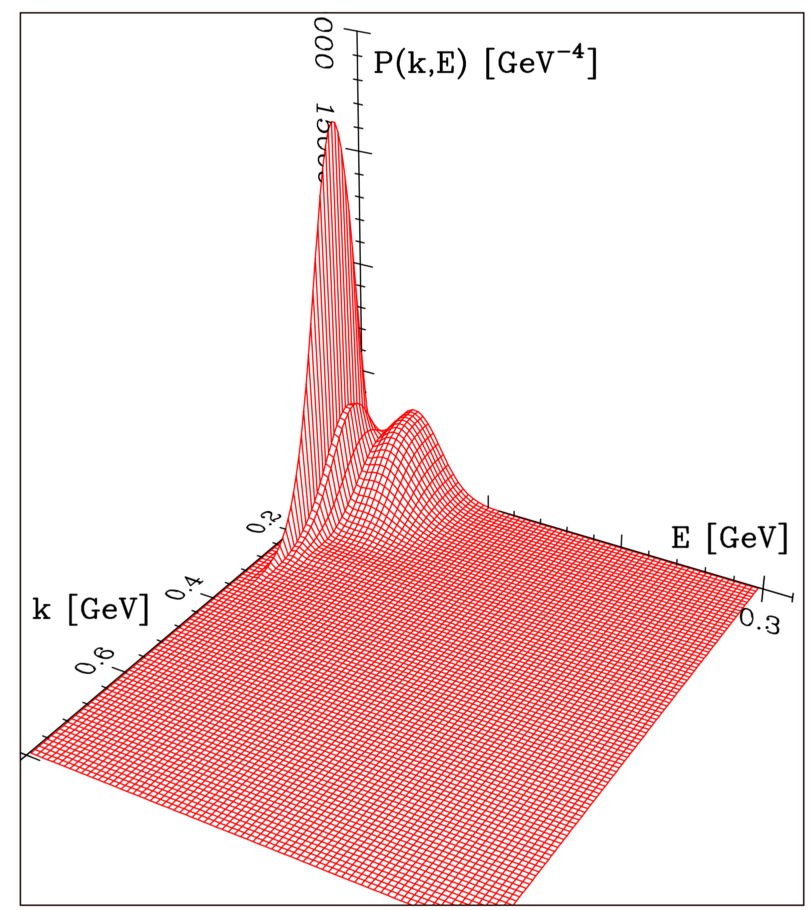

The intrinsic properties of the nucleus are described by the **Spectral Function**→ EFT and nuclear many-body methods

Extended Factorization Scheme

- Two-body currents are included rewriting the hadronic final state as

$$\boxed{|f\rangle \rightarrow |pp'\rangle_a \otimes |f_{A-2}\rangle}$$

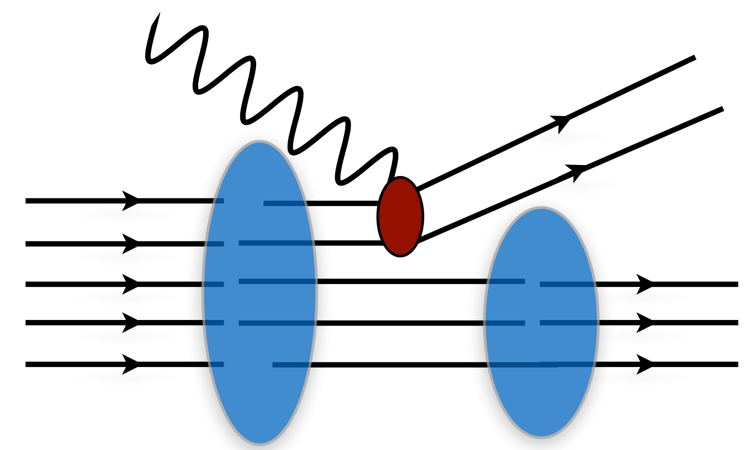

The hadronic tensor for two-body current processes reads

$$W^{\mu\nu}_{2\mathrm{b}}(\mathbf{q},\omega) \propto \int dE \frac{d^3k}{(2\pi)^3}\frac{d^3k'}{(2\pi)^3}\frac{d^3p}{(2\pi)^3} P_h(\mathbf{k},\mathbf{k}',E)\, 2\sum_{ij}\langle k\,k'|{j^{\mu}_{ij}}^{\dagger}|p\,p'\rangle_a$$
$$\times \langle p\,p'|j^{\nu}_{ij}|k\,k'\rangle \delta(\omega - E + 2m_N - e(\mathbf{p}) - e(\mathbf{p}')) .$$

✐ NR et al, Phys.Rev. C99 (2019) no.2, 025502

✐ NR et al, Phys. Rev. Lett. 116, 192501 (2016)

Relativistic two-body currents

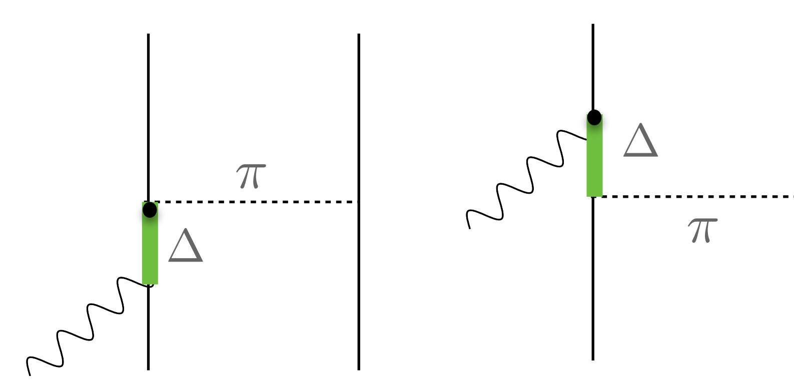

Dedicated code that **automatically** carries out the calculation of the **MEC spin-isospin matrix elements**, performing the integration using the Metropolis MC algorithm

Extended Factorization Scheme

- Production of real π in the final state

$$\boxed{|f\rangle \rightarrow |p_\pi p\rangle \otimes |f_{A-1}\rangle}$$

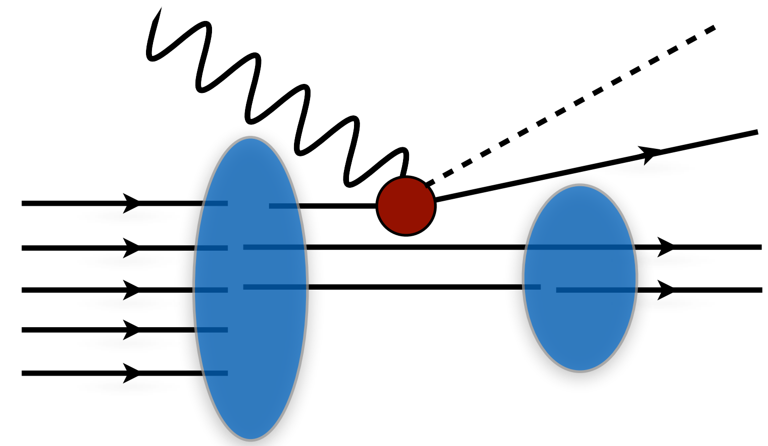

The hadronic tensor for two-body current processes reads

$$W^{\mu\nu}_{1\mathrm{b}1\pi}(\mathbf{q},\omega) \propto \int \frac{d^3k}{(2\pi)^3} dE\, P_h(\mathbf{k},E) \frac{d^3p_\pi}{(2\pi)^3} \sum_i \langle k|j_i^{\mu\,\dagger}|p_\pi p\rangle\langle p_\pi p|j_i^{\nu}|k\rangle$$
$$\times\, \delta(\omega - E + m_N - e(\mathbf{p}) - e_\pi(\mathbf{p}_\pi))$$

Pion production elementary amplitudes derived within the extremely sophisticated **Dynamic Couple Chanel approach**; includes meson baryon channel and nucleon resonances up to W=2 GeV

- The diagrams considered resonant and non resonant π production

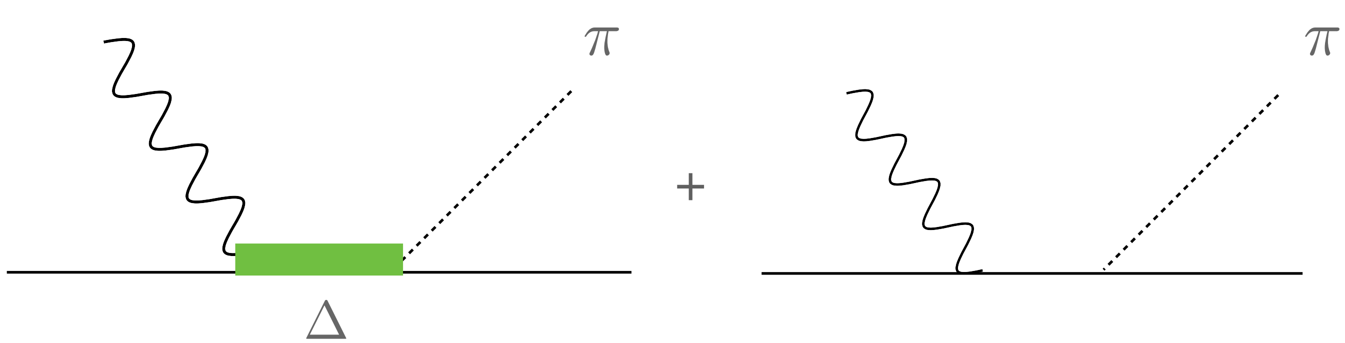

NR, et al, PRC100 (2019) no.4, 045503

H. Kamano et al, PRC 88, 035209 (2013)

S.X.Nakamura et al, PRD 92, 074024 (2015)

Electron and neutrino -^{12}C cross sections-SF

✐ NR, S. Nakamura, T.S.H. Lee, A. Lovato, PRC100 (2019) no.4, 045503

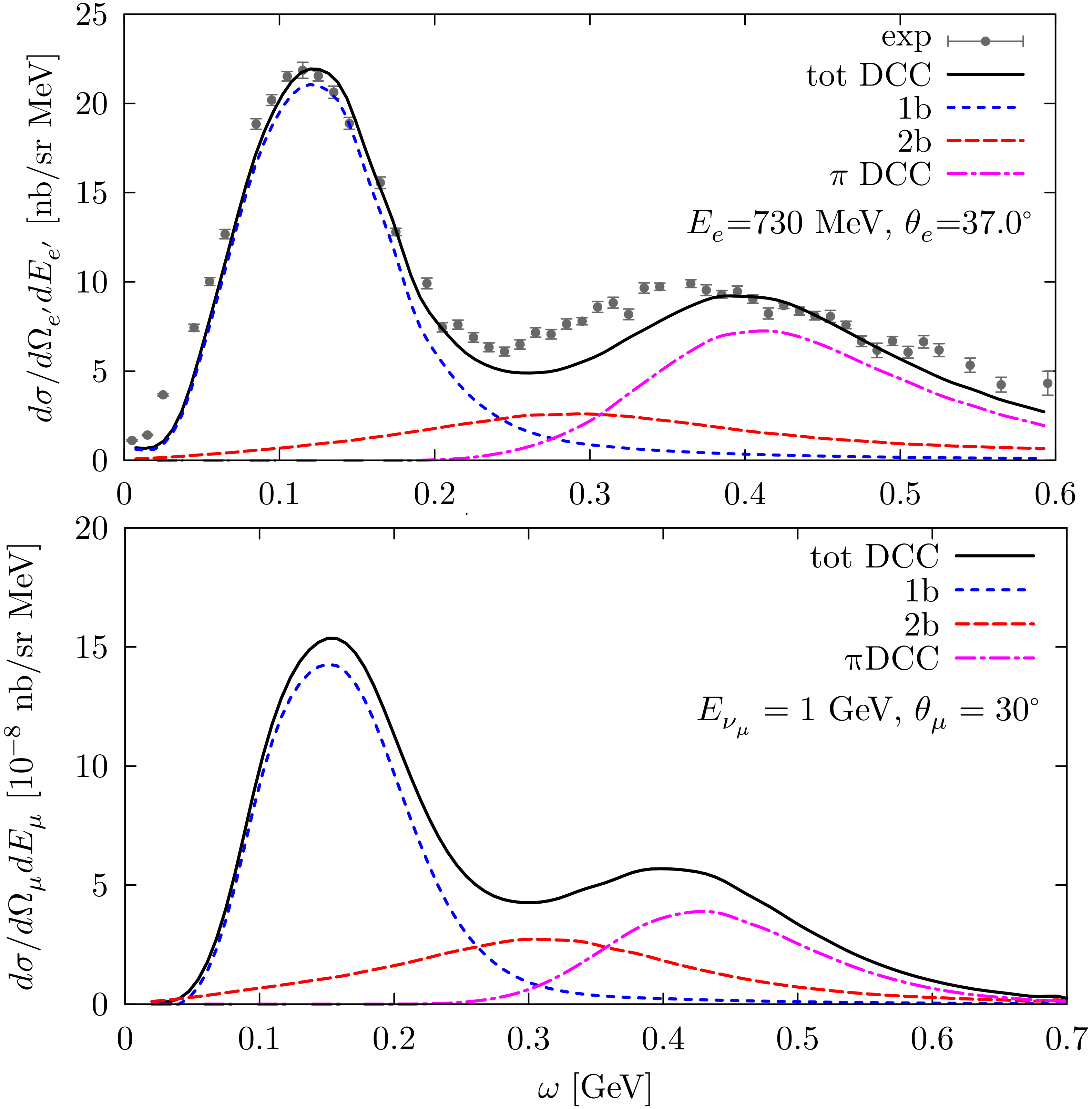

- We included in the Extended Factorization Scheme the **one-** and **two-body current** contributions and the **pion production** amplitudes.
- Good agreement with electron scattering data when all reaction mechanisms are included
- Ongoing calculation of flux folded cross sections

Electron and neutrino -^{12}C cross sections-SF

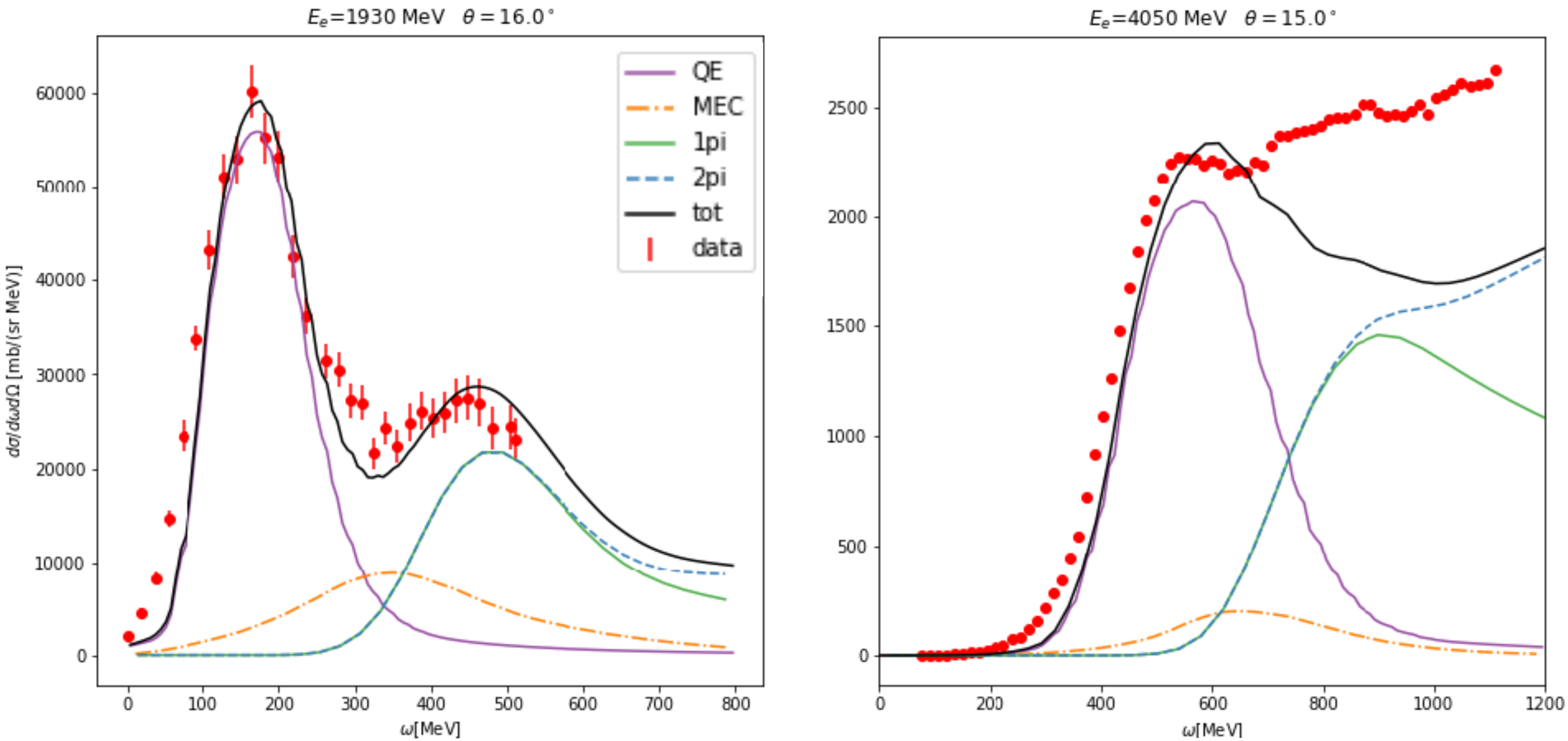

preliminary

- We included the DCC predictions for two π production
- We plan to tackle the DIS further extending the convolution approach: spectral function+nucleon pdf

A QMC based approach to intranuclear cascade

Figure by T. Golan

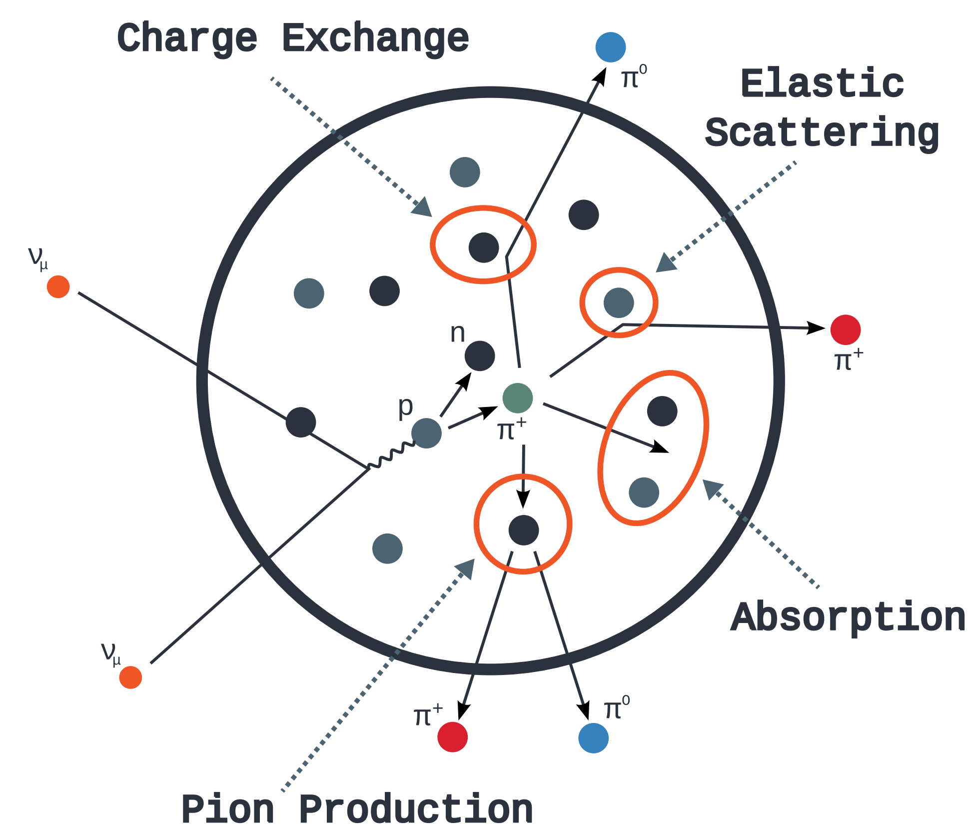

The propagation of **nucleons** through the **nuclear medium** is crucial in the analysis of electron-nucleus scattering and neutrino oscillation experiments.

Describing nucleons' propagation in the nuclear medium would in principle require a fully quantum-mechanical description of the hadronic final state.

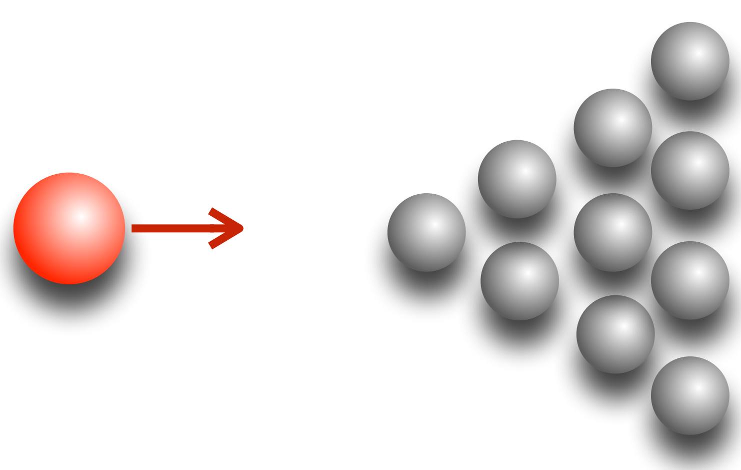

Due to its tremendous difficulty we follow a seminal work of Metropolis and develop a **semi-classical intranuclear cascade** (INC) that assume classical propagation between consecutive scatterings

J.Isaacson, W. Jay, P. Machado, A. Lovato, NR, arXiv:2007.15570

Sampling nucleon configurations

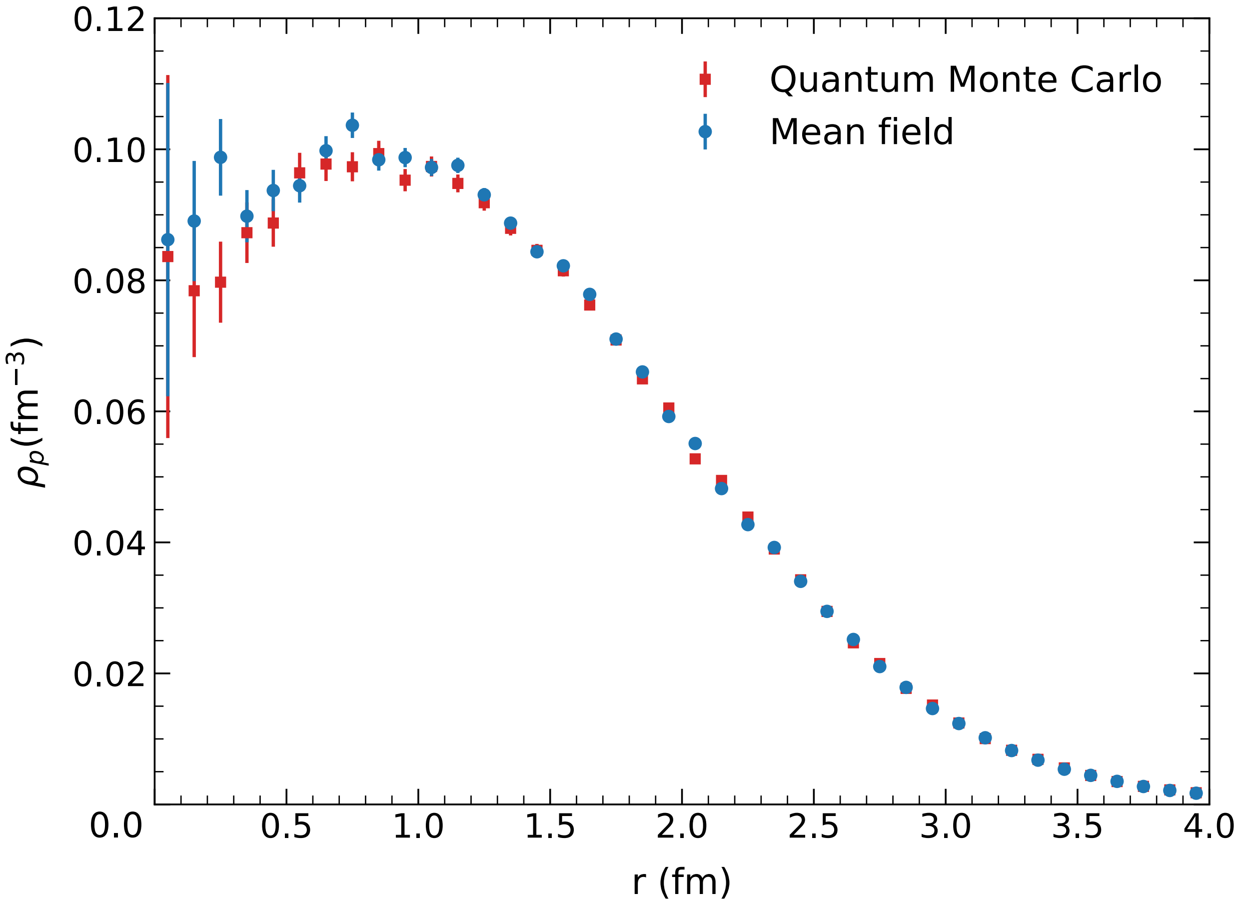

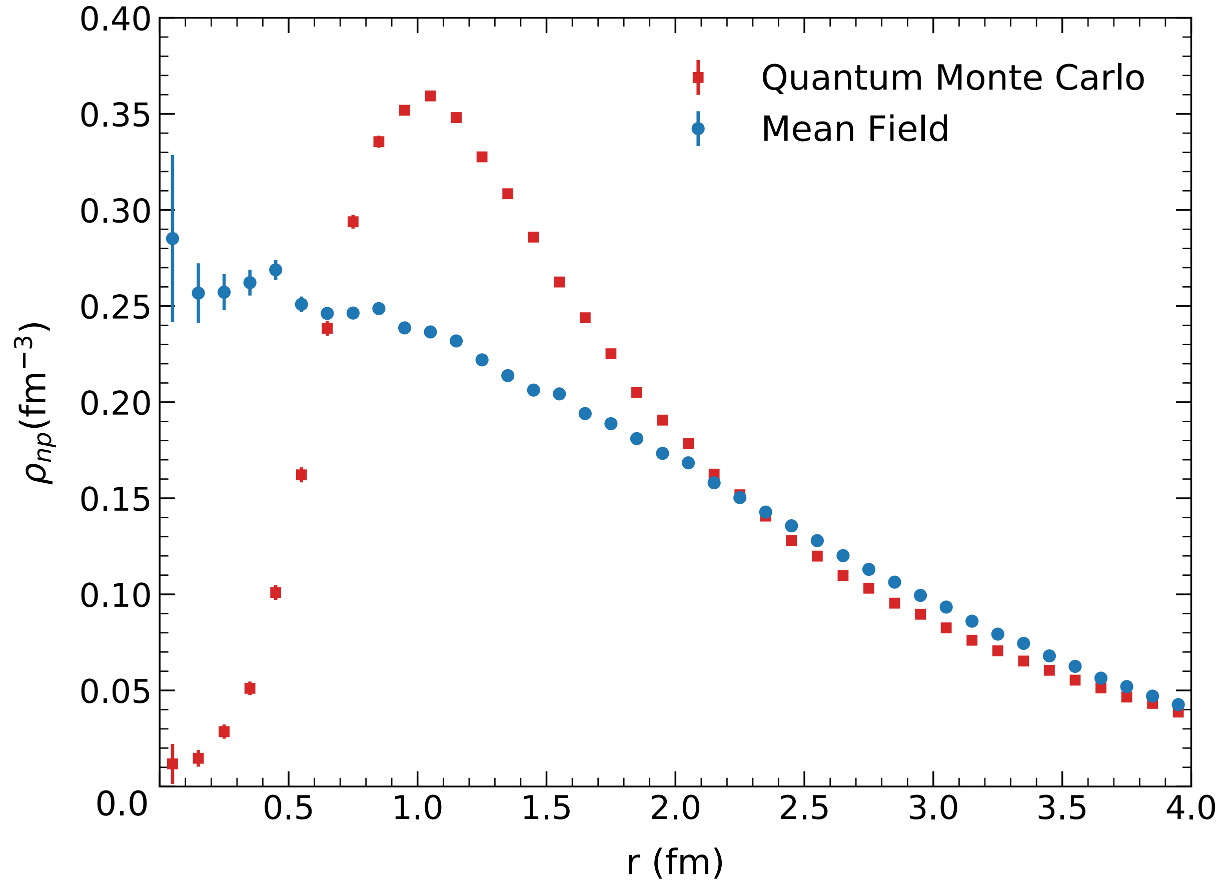

The nucleons' positions utilized in the INC are sampled from **36000 GFMC configurations**. For benchmark purposes we also sampled **36000 mean-field (MF) configurations** from the single-proton distribution.

The differences between GFMC and MF configurations are apparent when comparing the **two-body density distributions**: repulsive nature of two-body interactions reduced the probability of finding two particles close to each other

Probability of interaction

To check if an interaction between nucleons occurs an accept-reject test is performed on the closest nucleon according to a probability distribution.

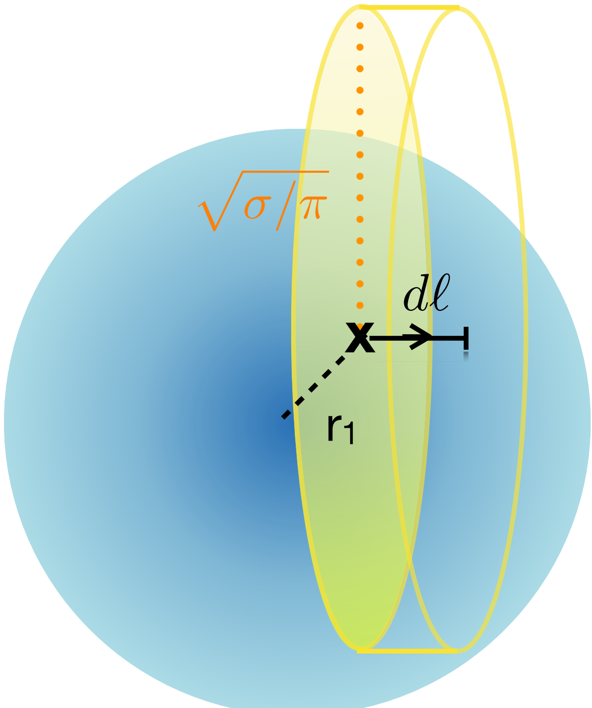

We use a **cylinder probability distribution**, this mimics a more classical billiard ball like system where each billiard ball has a radius
In addition we consider a **gaussian probability distribution**

For benchmark purposes, we also implemented the **mean free path approach**, routinely used in event generators

$$P = \sigma \bar{\rho} d\ell$$ where a constant density is assumed $$\rho(r_1) \sim \rho(r_1 + d\ell) \sim \bar{\rho}$$

we sample a number $0 \leq x \leq 1$ $\begin{cases} x < P & \checkmark \text{ the interaction occurred, check Pauli blocking} \\ x > P & \times \text{ the interaction DID NOT occur} \end{cases}$

Results: proton-Carbon cross section

Reproducing proton-nucleus cross section measurements is an important test of the accuracy of the INC model.

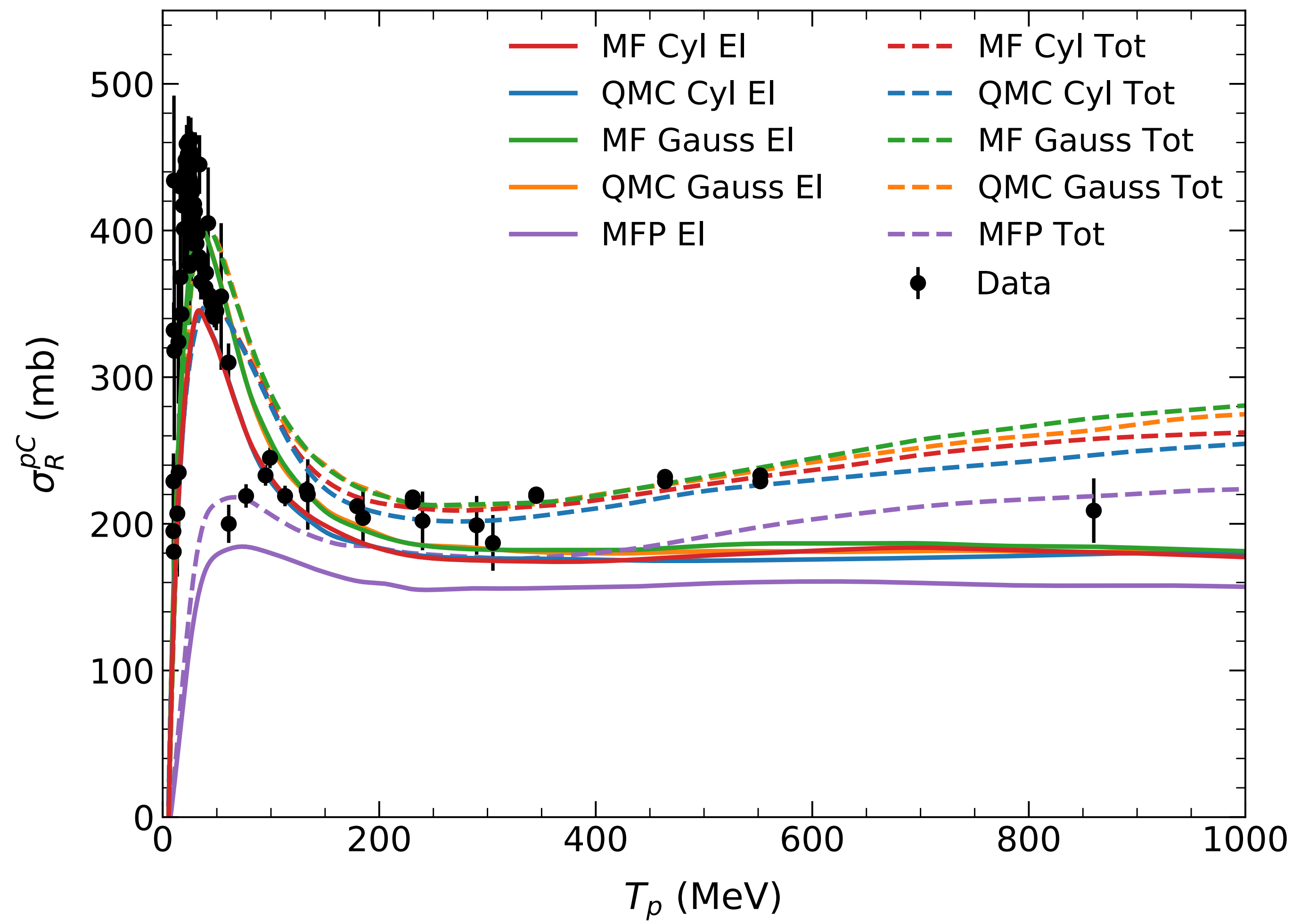

- We define a beam of protons with energy E, uniformly distributed over an area A.
- We propagate each proton in time and check for scattering at each step.
- The Monte Carlo cross section is defined as:

$$\sigma_{\mathrm{MC}} = A\frac{N_{\mathrm{scat}}}{N_{\mathrm{tot}}}$$

The **solid lines** have been obtained using the nucleon- nucleon cross sections from the **SAID database** in which only the **elastic contribution** is retained. The **dashed lines** used the **NASA parameterization** , which includes **inelasticities**.

Results: proton-Carbon cross section

The **Gauss** and **cylinder probability** distribution yield **similar results**

Large difference with the mean-free-path implementation: conceptual differences with respect to the previous cases

QMC and MF distribution lead to almost identical results: this observable does not depend strongly on correlations among the nucleons

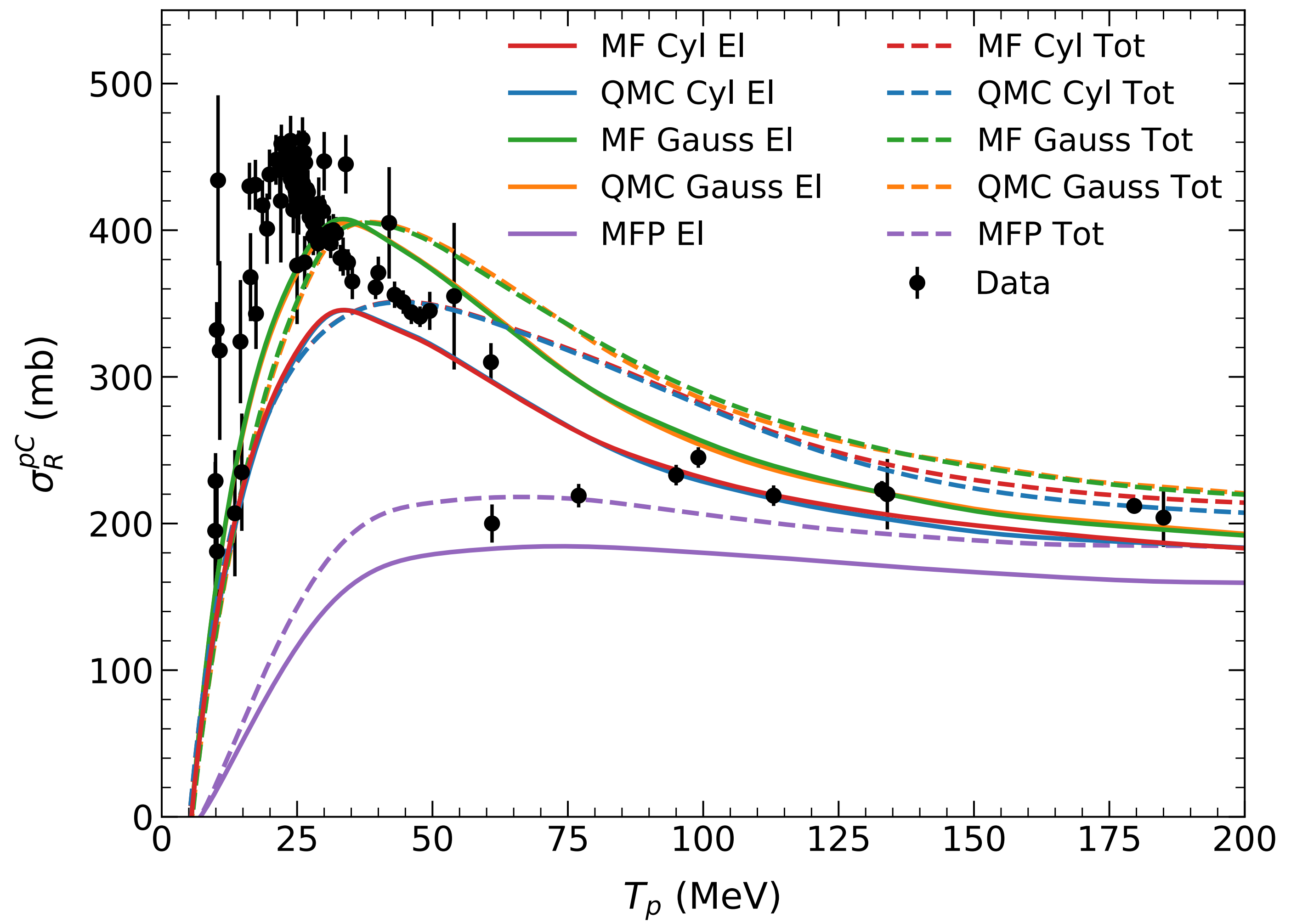

The **solid lines** have been obtained using the nucleon- nucleon cross sections from the SAID database in which only the **elastic contribution** is retained. The **dashed lines** used the NASA parameterization , which includes **inelasticities**.

Results: nuclear transparency

The **nuclear transparency** yields the average probability that a struck nucleon leaves the nucleus without interacting with the spectator particles

Nuclear transparency is **measured in (e,e'p) scattering** experiments

Simulation: we randomly sample a nucleon with kinetic energy Tp and propagate it through the nuclear medium

$$T_{\mathrm{MC}} = 1 - \frac{N_{\mathrm{hits}}}{N_{\mathrm{tot}}}$$

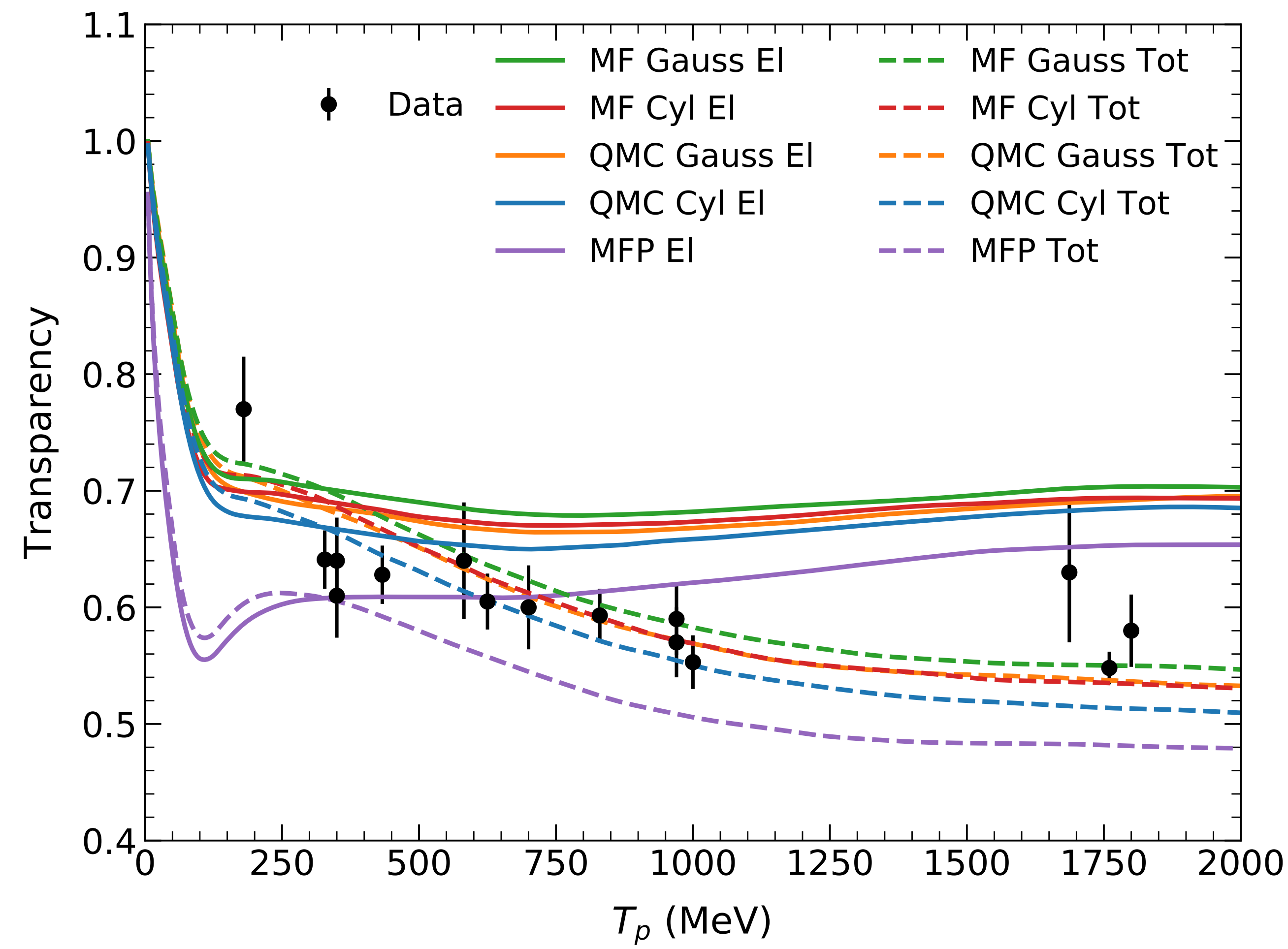

Gaussian and cylinder curves are consistent and correctly reproduces the data. Correlations do not seem to play a big role.

Results: correlation effects

Histograms of the **distance traveled** by a struck particle **before the first interaction** takes place for different values of the interaction cross section

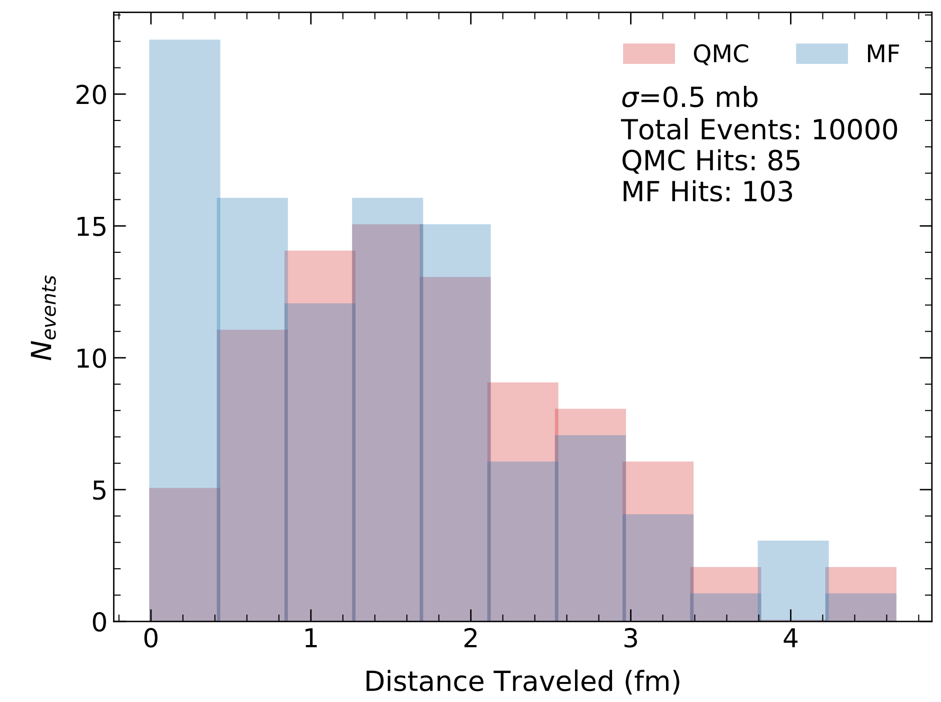

When using **QMC configurations**, the hit nucleon is surrounded by a short-distance **correlation hole**: expected to propagate freely for ~ 1 fm before interacting

For **σ=0.5 mb** the **MF distribution peaks toward smaller distances than the QMC one**: originates from the repulsive nature of the nucleon-nucleon potential

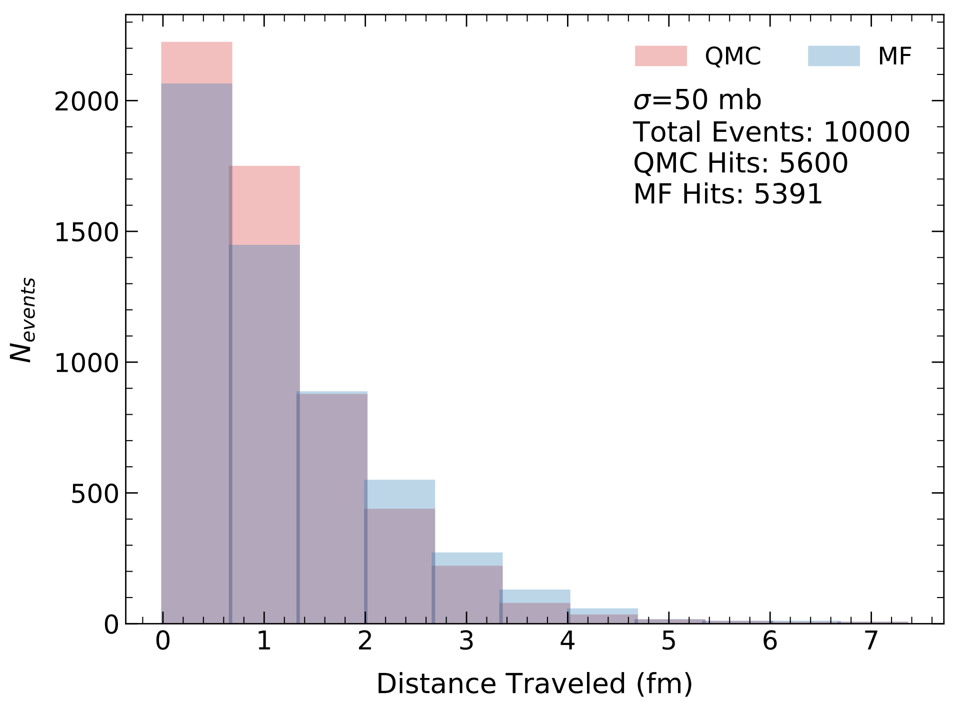

For **σ=50 mb** large cylinder, **MF and QMC distributions become similar.** The propagating particle is less sensitive to the local distribution of nucleons and more sensitive to the integrated density over a larger volume, reducing the effect of correlations

Future theory efforts

✐ S.Gandolfi, D.Lonardoni, et al, *Front.Phys.* 8 (2020) 117

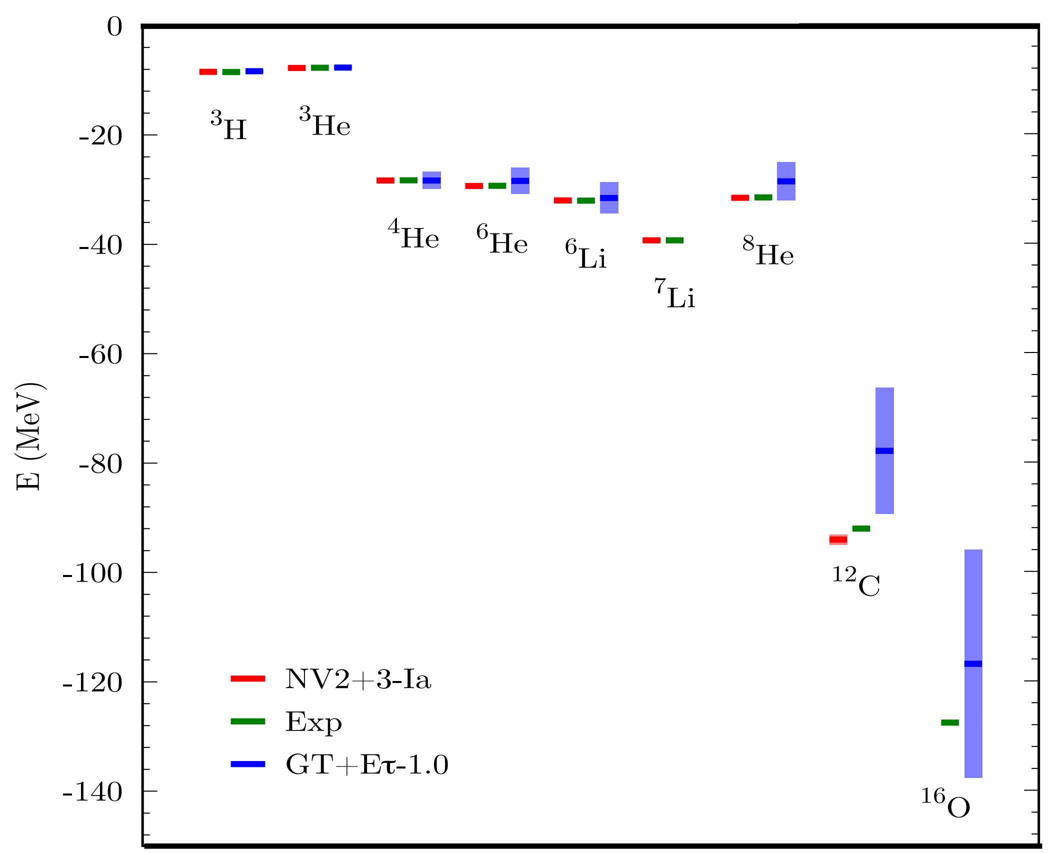

Using more approximate methods, **calculation of lepton-Ar cross sections.** **Extend** the factorization scheme to the **DIS**

Intranuclear cascade: include **π degrees of freedom**: π production, absorption and elastic scattering as well as **in medium corrections**

Theoretical uncertainty estimate: truncation of the chiral expansion and statistical uncertainty of the ab-initio method

Devise an **hybrid QMC** approach able to describe larger nuclei such as ^{16}O and use machine learning algorithms to obtain cross sections

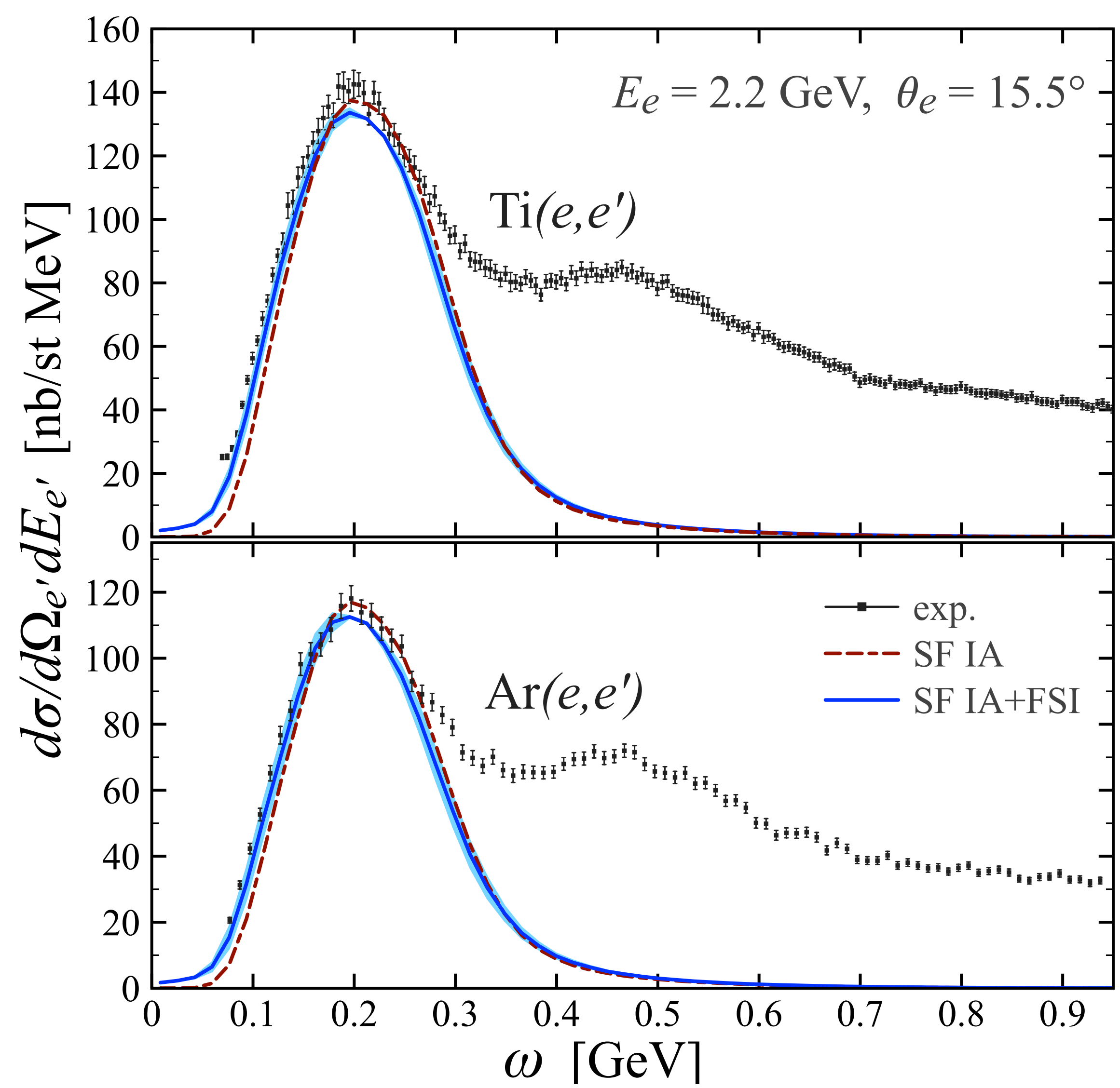

✐ C.Barbieri, NR, V.Somà, PRC 100 (2019) 6, 062501

Thank you for your attention!

Extension to Deep Inelastic Scattering

I plan to extend the Factorization scheme to **treat the DIS region**

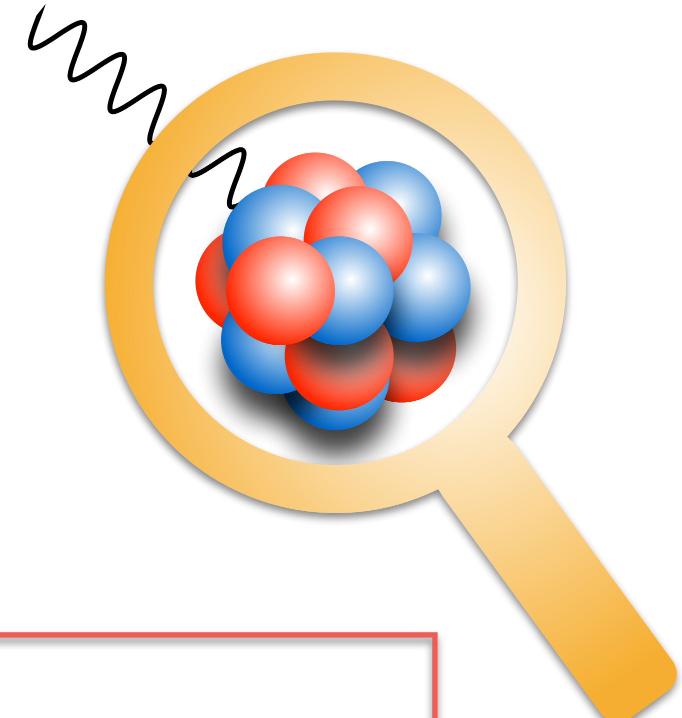

$$d\sigma_A = \int dE\, d^3k\, d\sigma_N\, P(\mathbf{k}, E)$$

$$d\sigma_N \propto W_2(\omega, q^2) cos^2\frac{\theta}{2} + 2W_1(\omega, q^2) sin^2\frac{\theta}{2}$$

$$W_1^p = -\frac{q^2}{4m^2} G_{M_p}^2 \delta(\omega + \frac{q^2}{2m})$$

$$W_2^p = \frac{G_{E_p}^2 - q^2/(4m^2) G_{M_p}^2}{1 - q^2/(4m^2)} \delta(\omega + \frac{q^2}{2m})$$

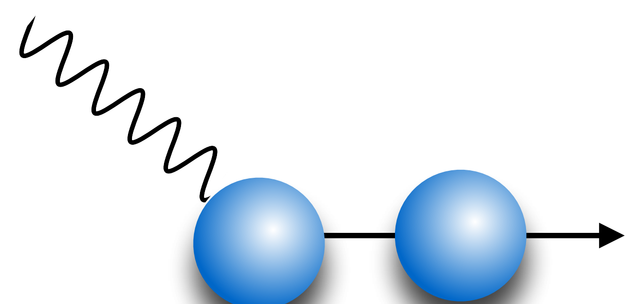

$$Q^2 \to \infty, \;\; \omega \to \infty$$

$$\omega W_2(\omega, q^2) \to F_2(x) = \sum_i e_i^2 x f_i(x)$$

$$m W_1(\omega, q^2) \to F_1(x) = \frac{1}{2x} F_2(x)$$

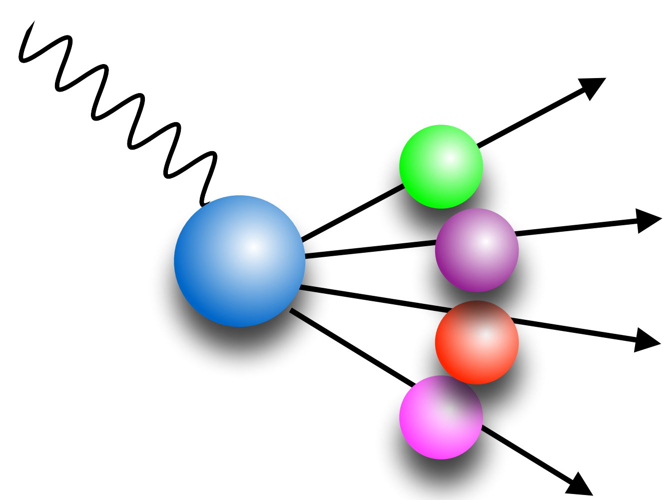

Integral Transform Techniques

- Nuclear responses obtained with QMC techniques (more in detail Greens' Function Monte Carlo)

$$R_{\alpha\beta}(\omega, \mathbf{q}) = \sum_f \langle 0|J_\alpha^\dagger(\mathbf{q})|f\rangle\langle f|J_\beta(\mathbf{q})|0\rangle\delta(\omega - E_f + E_0)$$

Valuable information can be obtained from the integral transform of the response function

$$E_{\alpha\beta}(\sigma, \mathbf{q}) = \int d\omega K(\sigma, \omega) R_{\alpha\beta}(\omega, \mathbf{q}) = \langle\psi_0|J_\alpha^\dagger(\mathbf{q})K(\sigma, H - E_0)J_\beta(\mathbf{q})|\psi_0\rangle$$

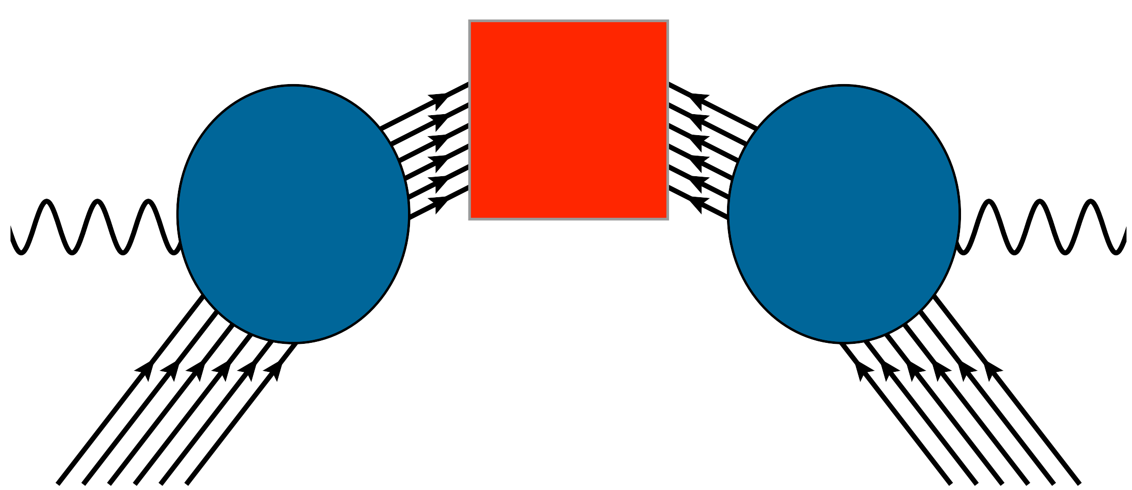

Integral Transform Techniques

$E(\sigma, \mathbf{q}) \xrightarrow{?} R(\omega, \mathbf{q})$

Inverting the integral transform is a complicated problem

$E_{\alpha\beta}(\tau, \mathbf{q}) \longrightarrow R_{\alpha\beta}(\omega, \mathbf{q})$

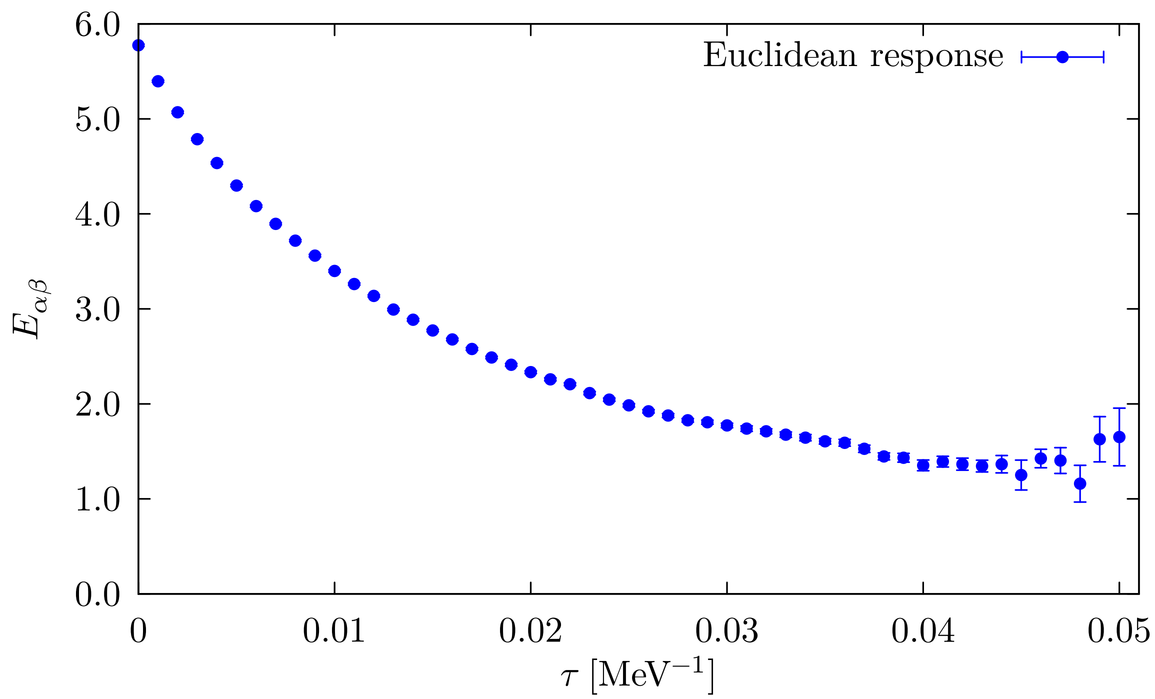

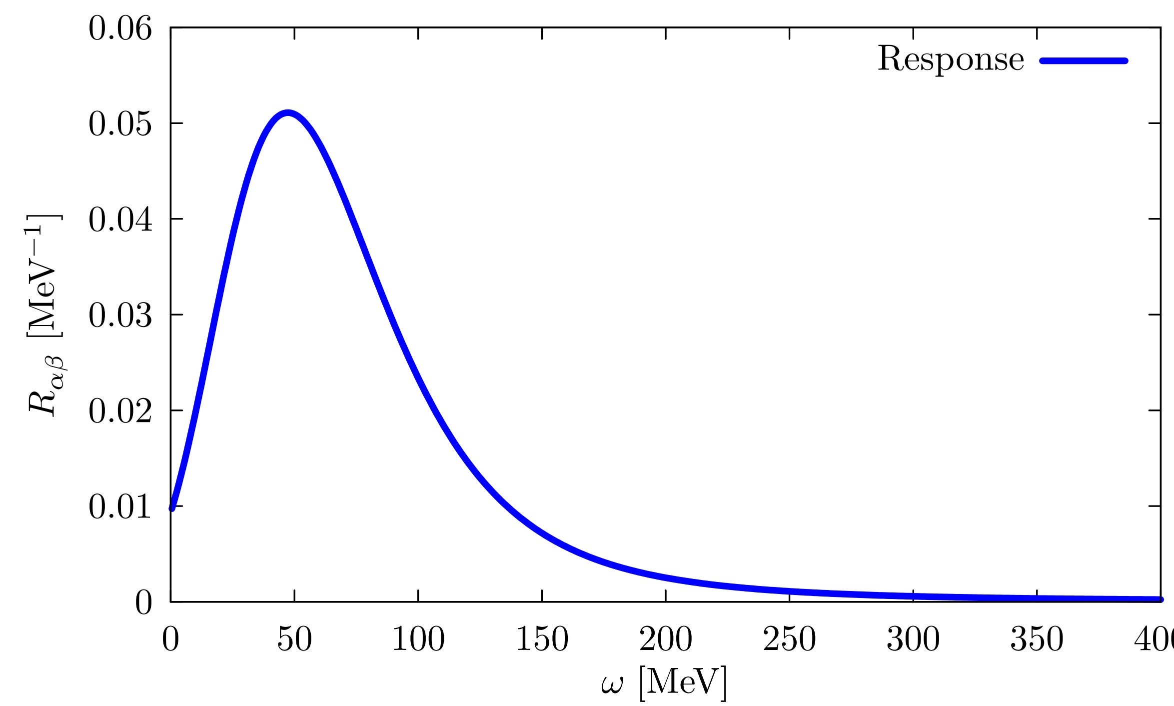

Current solution for the quasielastic region: Maximum Entropy Techniques

A. Lovato et al, Phys.Rev.Lett. 117 (2016), 082501, Phys.Rev. C97 (2018), 022502

We are now exploring new strategies, based on **machine learning techniques**, to improve the accuracy of the inversion and to better estimate the associated uncertainties

Integral Transform Techniques

- Nuclear responses obtained with QMC techniques (more in detail Greens' Function Monte Carlo)

$$R_{\alpha\beta}(\omega,\mathbf{q}) = \sum_f \langle 0|J_\alpha^\dagger(\mathbf{q})|f\rangle\langle f|J_\beta(\mathbf{q})|0\rangle\delta(\omega - E_f + E_0)$$

Valuable information can be obtained from the integral transform of the response function

$$E_{\alpha\beta}(\sigma,\mathbf{q}) = \int d\omega K(\sigma,\omega)R_{\alpha\beta}(\omega,\mathbf{q}) = \langle\psi_0|J_\alpha^\dagger(\mathbf{q})K(\sigma,H-E_0)J_\beta(\mathbf{q})|\psi_0\rangle$$

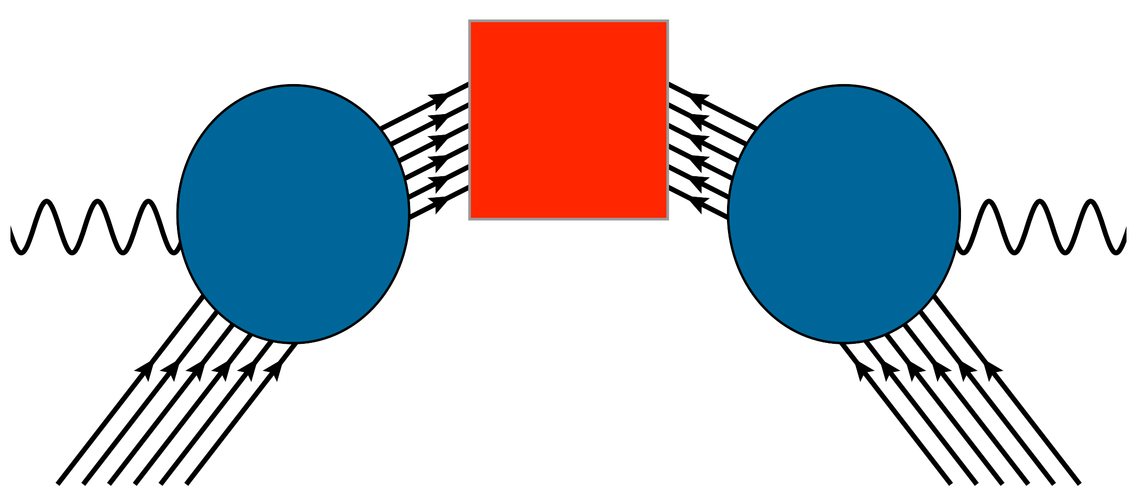

Integral Transform Techniques

$E(\sigma, \mathbf{q}) \xrightarrow{?} R(\omega, \mathbf{q})$

Inverting the integral transform is a complicated problem

$E_{\alpha\beta}(\tau, \mathbf{q}) \longrightarrow R_{\alpha\beta}(\omega, \mathbf{q})$

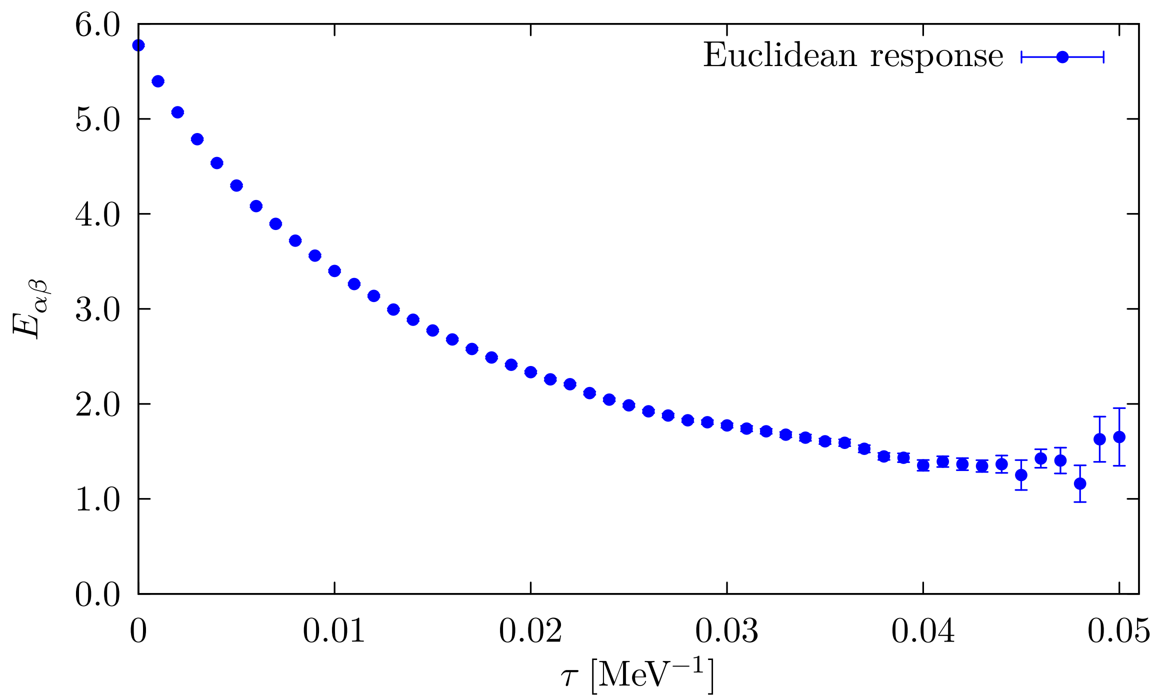

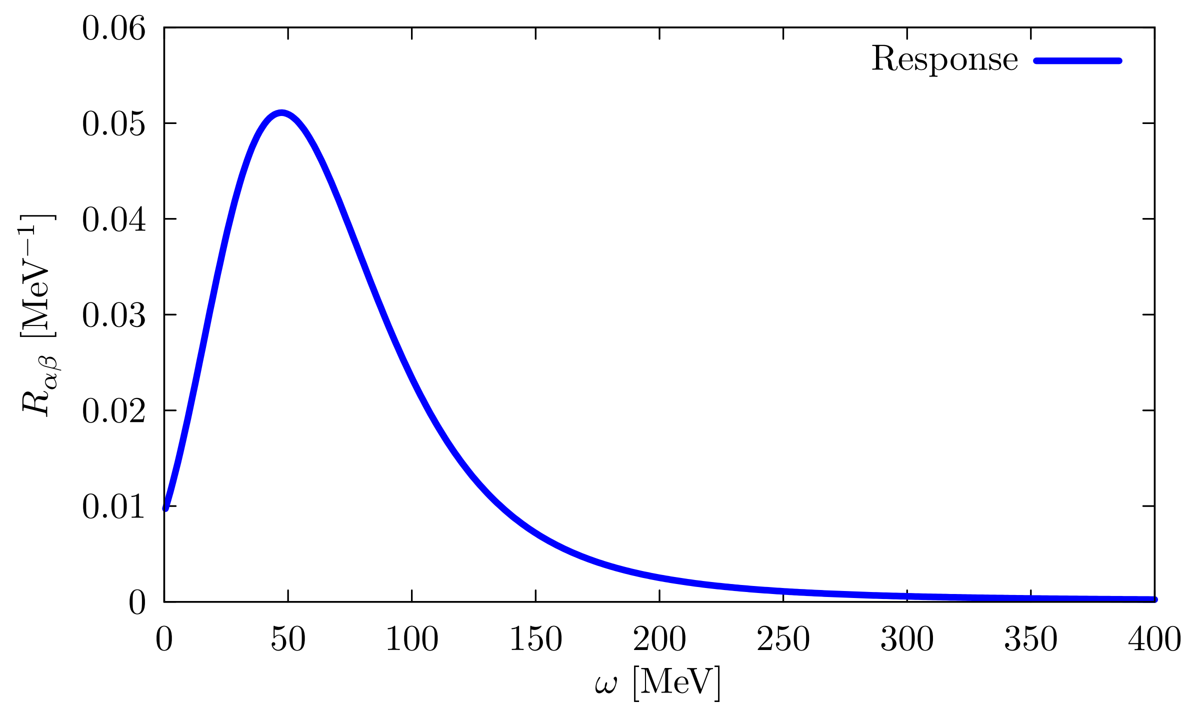

Current solution for the quasielastic region: Maximum Entropy Techniques

A. Lovato et al, Phys.Rev.Lett. 117 (2016), 082501, Phys.Rev. C97 (2018), 022502

We are now exploring new strategies, based on **machine learning techniques**, to improve the accuracy of the inversion and to better estimate the associated uncertainties

Predicting Argon cross sections

- ^{40}Ar(e,e') and ^{48}Ti(e,e') cross sections w-w/o FSI

✐ C. Barbieri, NR, and V. Somà, arXiv:1907.01122

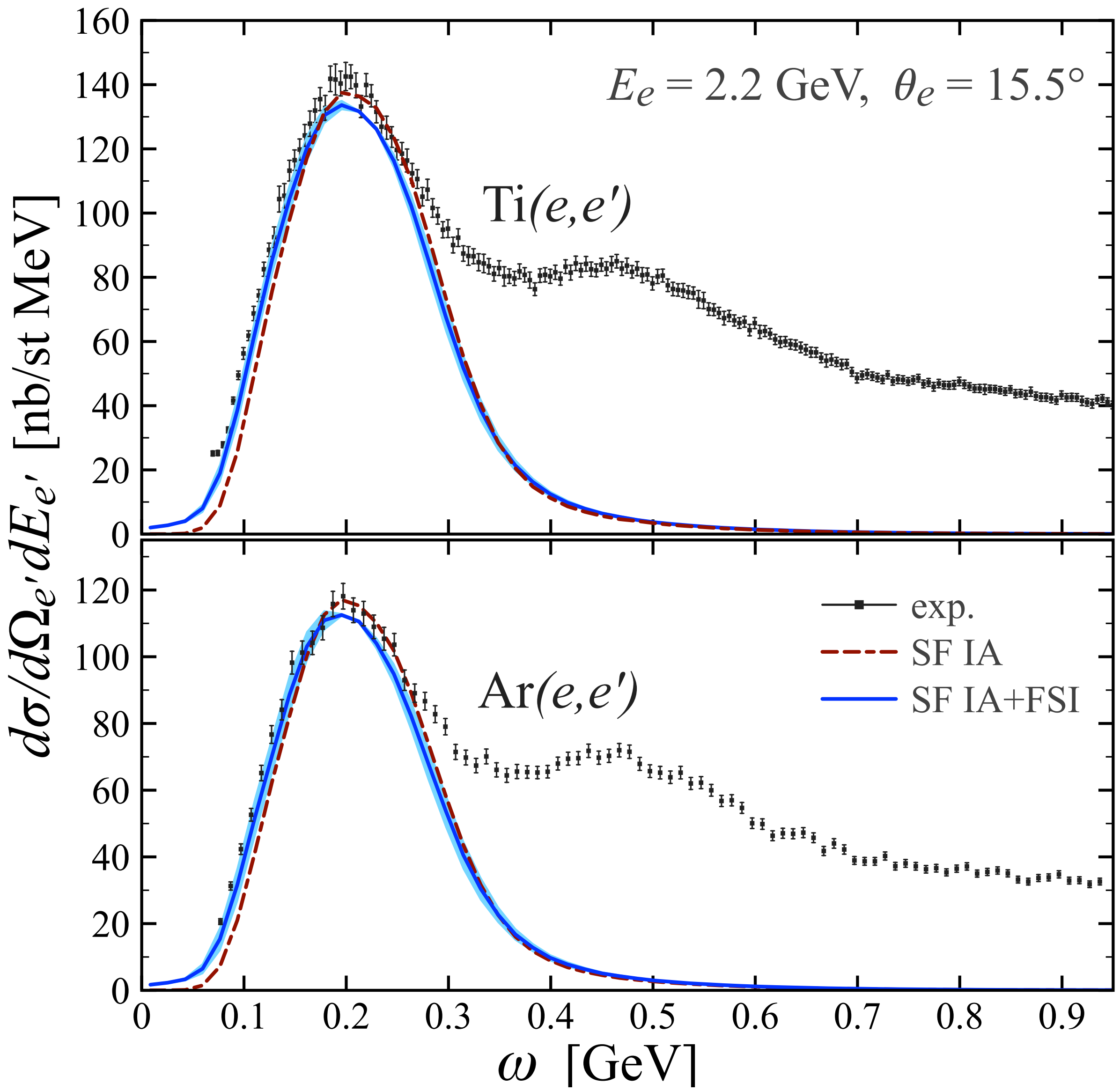

- Charge current and neutral current ν_μ scattering on ^{12}C and Ar for E_{ν_μ} =1 GeV

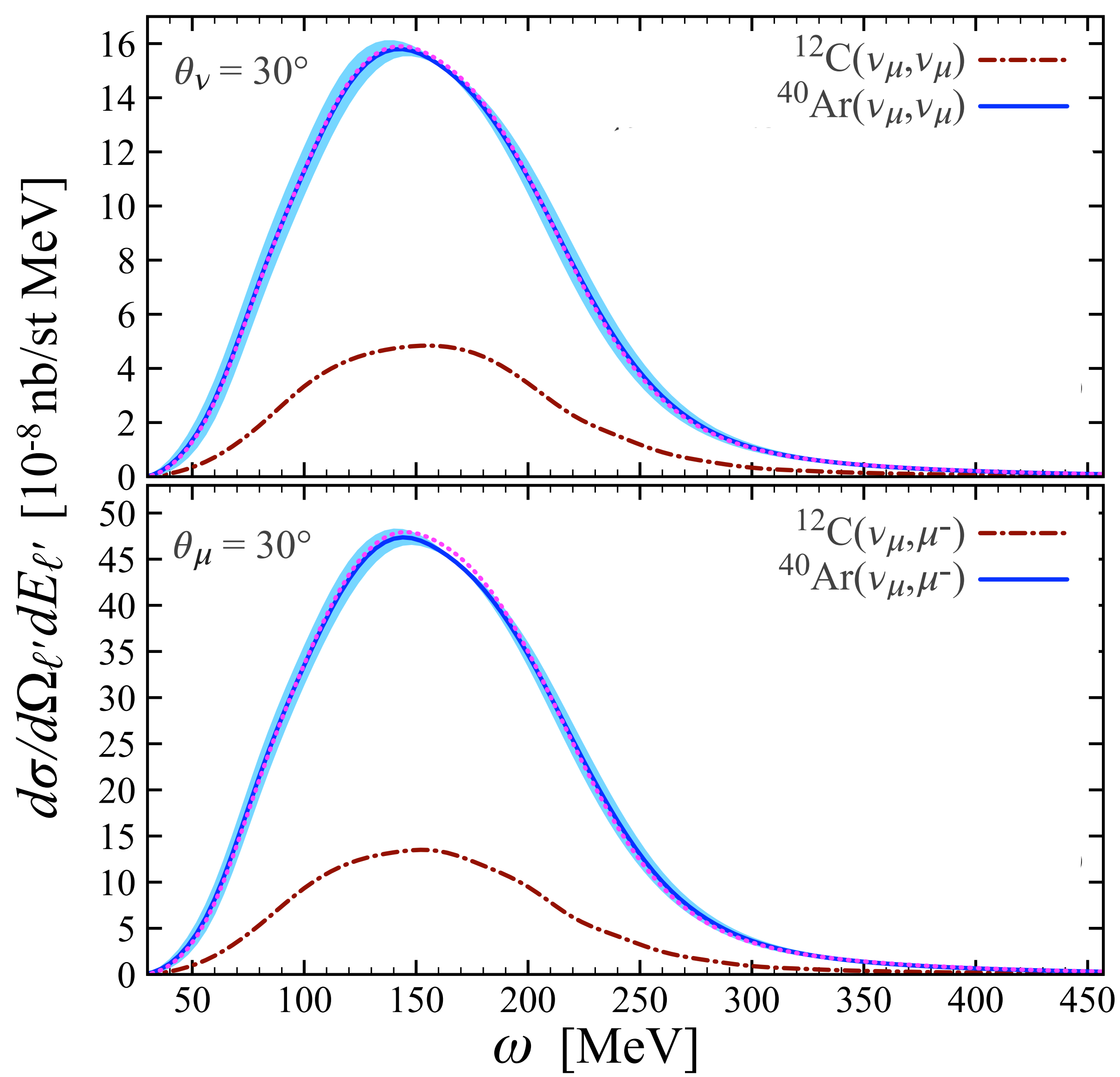

- The band comes from a **first estimate of the uncertainty on the spectral function** calculation obtained by varying the model-space and the harmonic oscillator frequency

Global Fermi gas: independent particles

Protons and neutrons are considered as **moving freely** within the nuclear volume

Simple picture of the nucleus: only **statistical correlations** are retained (Pauli exclusion principle)

The energy of the highest occupied state is the **Fermi energy: E_F, B' constant binding energy**

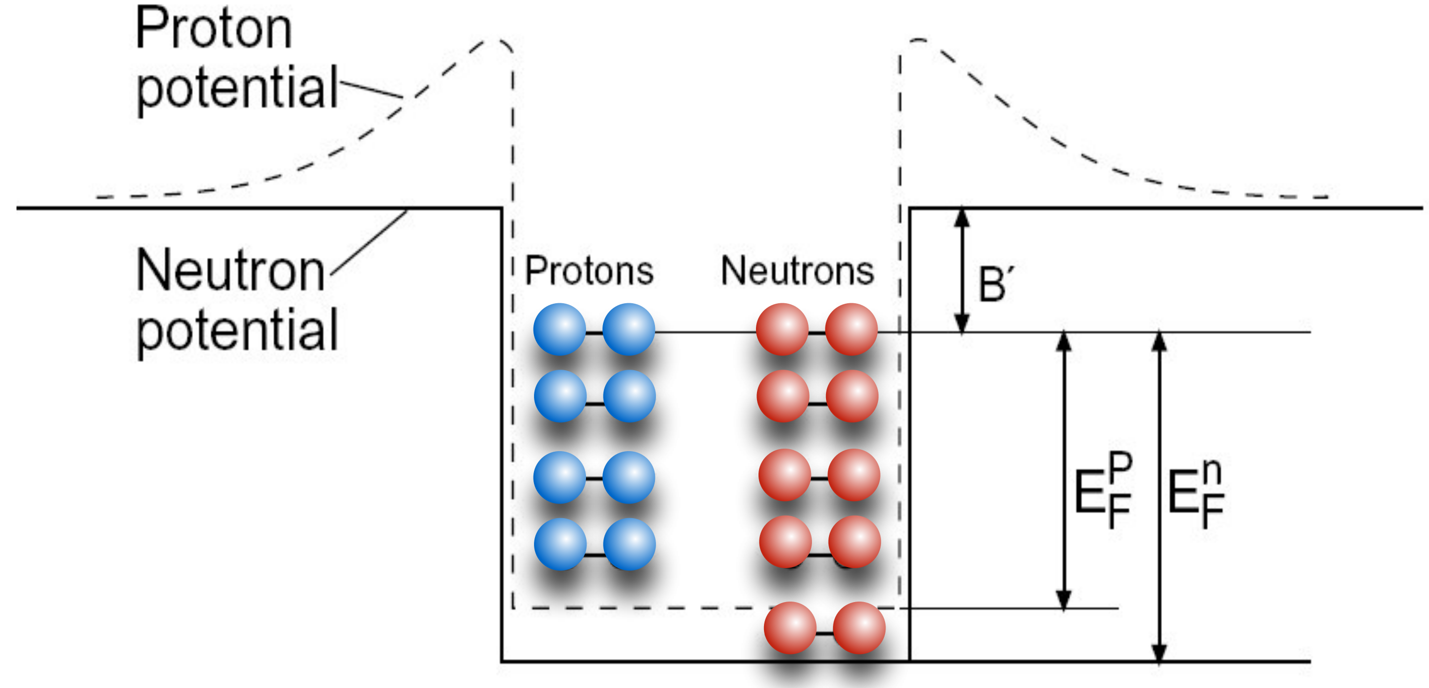

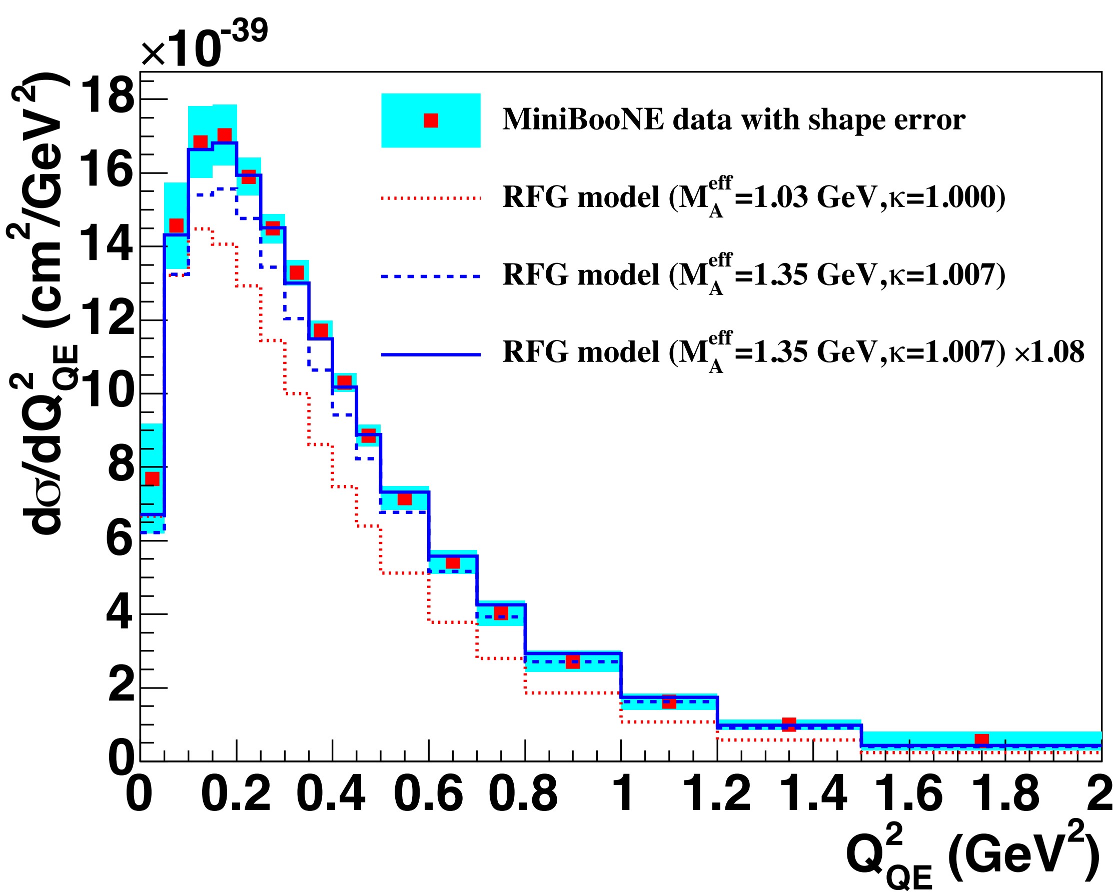

MiniBooNE collaboration, PRD 81 (2010) 092005

The Global Fermi gas model has been widely used in comparisons of neutrino scattering data.

MiniBooNE data analysis requires M_A~1.35 GeV to reproduce the data: incompatible with former measurements in bubble chamber: M_A~1.03 GeV

Nuclear effects can explain the axial mass puzzle

The Spectral Function of finite nuclei

- Two different many-body methods to compute the spectral function of finite nuclei

  - Correlated Basis Function: the SF obtained within CBF and using the Local Density Approximation

$$P_{LDA}(\mathbf{k},E) = P_{MF}(\mathbf{k},E) + P_{corr}(\mathbf{k},E)$$

$$P_{MF}(\mathbf{k},E) \rightarrow \boxed{\sum_n Z_n |\phi_n(\mathbf{k})|^2 F_n(E-E_n)}$$

$$P_{corr}(\mathbf{k},E) \rightarrow \boxed{\int d^3r P^{NM}_{corr}(\mathbf{k},E;\rho=\rho_A(r))}$$

O. Benhar et al, Nucl. Phys. A505, 267 (1989)

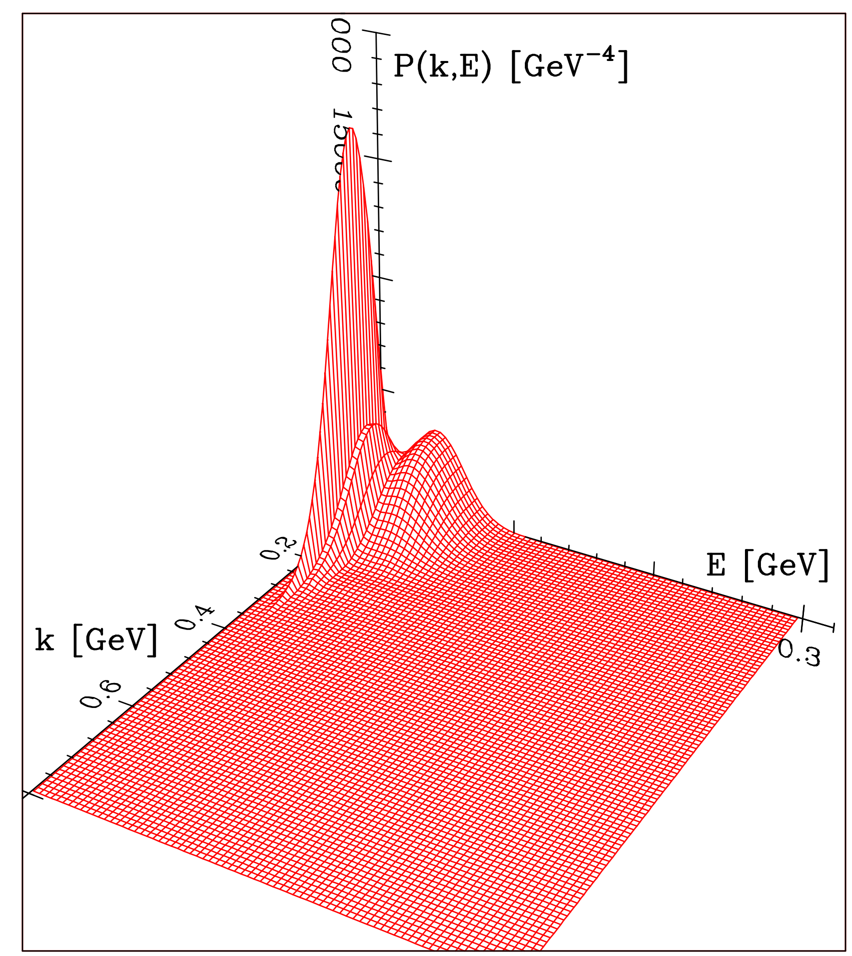

  - Self Consistent Green's Function : ab-initio method, the SF obtained solving the Dyson Equation for the corresponding propagator

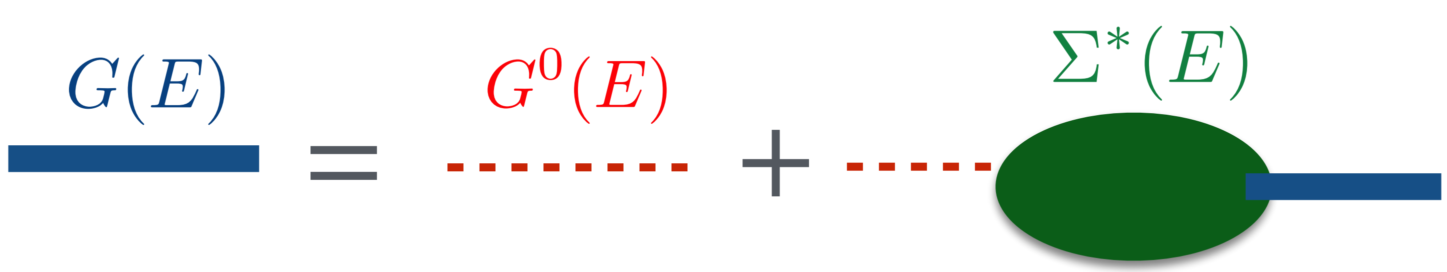

V. Somà et al, PRC87 (2013) no.1, 011303

- Results currently available are for electron and neutrino scattering on:

  ^{4}He, ^{12}C, ^{16}O within the CBF

  ^{12}C, ^{16}O, Ca,Ti and Ar within the SCGF

The CBF Spectral Function of finite nuclei

- Within the Fermi Gas model we can define the SF as:

$$P^{\rm FG}(\mathbf{k}, E) = \delta(E - \epsilon_B)\theta(p_F - |\mathbf{k}|)$$

- High energy and momentum correlated pairs

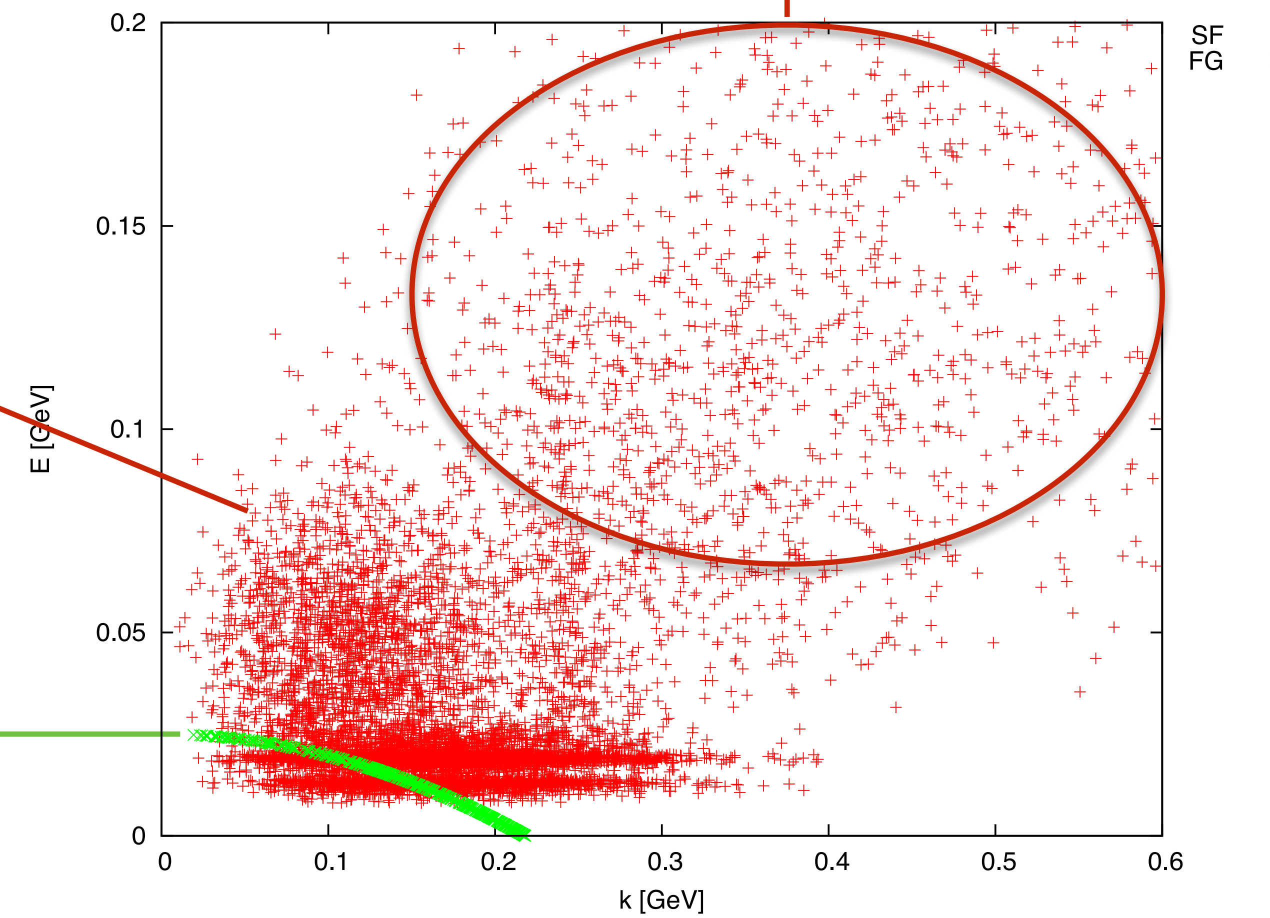

Realistic SF: 80% shell model picture, 20% SRC

Fermi gas contribution

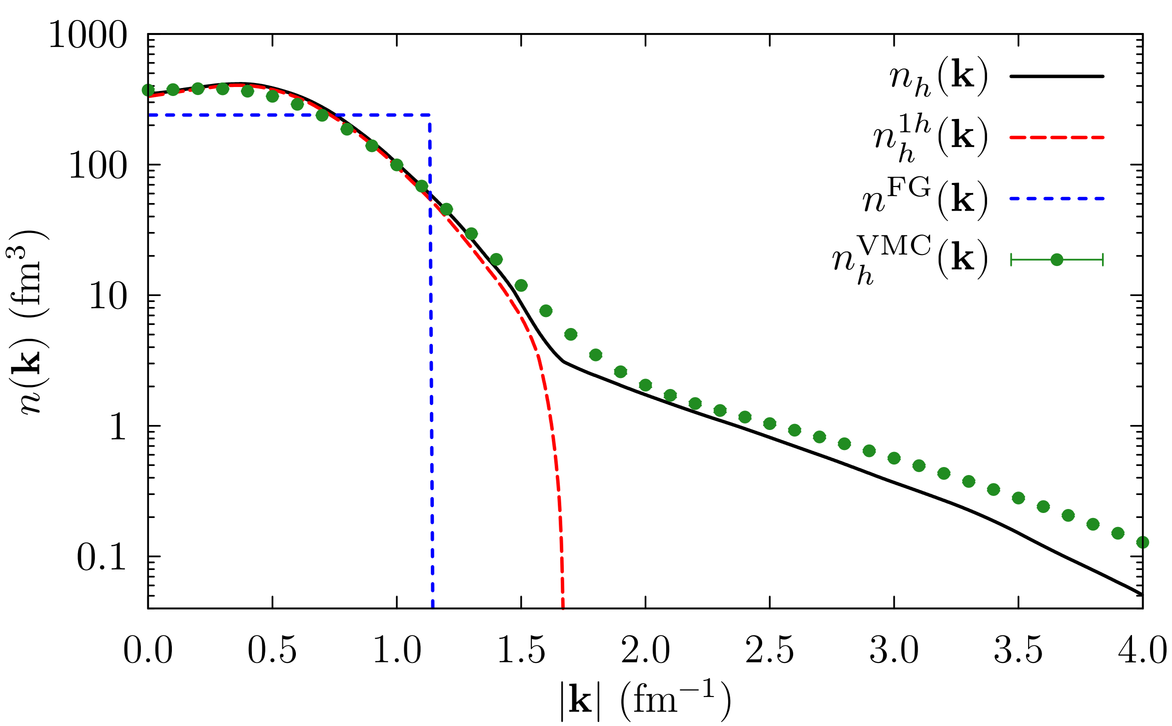

- VMC: exact calculation of the momentum distribution including SRC pairs
- CBF: calculation
- 1h corresponds to the MF, rapidly drops
- FG: unrealistic momentum distribution, totally missing the high momentum component

Two-body (phenomenological) potential

Realistic local, configuration-space potential are controlled by **thousands np and pp scattering data** below 350 MeV of the Nijmegen and Granada databases

Nuclear potentials are strongly spin-isospin dependent. **Argonne $\mathbf{v_{18}}$** can be written as

$$v_{18}(r_{ij}) = v_{ij}^{\gamma} + v_{ij}^{\pi} + v_{ij}^{I} + v_{ij}^{S} = \sum_{p=1}^{18} v^p(r_{ij}) O_{ij}^p$$

- Static part $O_{ij}^{p=1-6} = (1, \sigma_{ij}, S_{ij}) \otimes (1, \tau_{ij})$
- Spin-orbit $O_{ij}^{p=7-8} = \mathbf{L}_{ij} \cdot \mathbf{S}_{ij} \otimes (1, \tau_{ij})$

Some of the Feynman diagrams effectively included in the Argonne potential